TECHNICAL UNIVERSITY OF LIBEREC
Faculty of Mechatronics, Informatics
and Interdisciplinary Studies

CHARACTERIZATION OF BEHAVIOUR AND TRANSFORMATION OF NANOMATERIALS IN ENVIRONMENTALLY RELEVANT MEDIA

Diploma thesis

Study Programme: N3942 – Nanotechnology
Branch of Study: 3942T002 – Nanomaterials

Author: **Bc. Martin Štryncl**
Supervisor: RNDr. Alena Ševců, Ph.D.

Liberec 2014

TECHNICKÁ UNIVERZITA V LIBERCI
Fakulta mechatroniky, informatiky a mezioborových studií
Akademický rok: **2013/2014**

ZADÁNÍ DIPLOMOVÉ PRÁCE

(PROJEKTU, UMĚLECKÉHO DÍLA, UMĚLECKÉHO VÝKONU)

Jméno a příjmení:	**Bc. Martin Štryncl**
Osobní číslo:	**M12000007**
Studijní program:	**N3942 Nanotechnologie**
Studijní obor:	**Nanomateriály**
Název tématu:	**Charakterizace nanomateriálů z hlediska jejich chování a transformace v environmentálně relevantních prostředích**
Zadávající katedra:	**Ústav nových technologií a aplikované informatiky**

Zásady pro vypracování:

1. Vypracovat literární rešerši na téma: Charakterizace nanomateriálů z hlediska jejich chování a transformace v environmentálně relevantních prostředích. (Zdrojem informací budou především vědecké články dostupné na běžných vyhledávačích: Web of Science, Scopus, Google Scholar).
2. Vybrat nejméně dva typy nanočástic, jejichž chování bude testované v environmentálně relevantních prostředích, jako je např. povrchová voda (řeka, přehradní nádrž) nebo podpovrchová znečištěná voda (ze sanačního vrtu).
3. Sledovat důležité vlastnosti nanočástic z hlediska jejich chování ve skutečném životním prostředí (vliv na velikost, aglomeraci, zeta potenciál, morfologii atd.) Důraz bude kladený na stárnutí nanočástic a sledování změn jejich vlastností.
4. Provést experimenty s chováním nanočástic v environmentálně relevantních, ale extrémních podmínkách (pH, teplota, ORP). Zde se budou sledovat stejné parametry jako v bodu 3.
5. Součástí studia je stáž v Centre for BioNano Interactions v Dublinu pod vedením prof. Kennetha Dawsona. Zde se student seznámí s analytikou nanočástic pomocí diskové centrifugy CPS a provede experimenty na porovnání velikosti nanočástic v různých typech prostředí.

Rozsah grafických prací:	**dle potřeby**
Rozsah pracovní zprávy:	**60 stran**
Forma zpracování diplomové práce:	**tištěná/elektronická**

Seznam odborné literatury:

[1] ČERNÍK, M. a kol.: Chemicky podporované in-situ sanační technologie. 1. vyd. Praha: Vydavatelství VŠCHT Praha, 2010. ISBN 978-80-7080-767-5.
[2] NAVARRO, D. A. 2012: Investigating fate and transport behavior of cadmium selenide QD and transition metal oxide nanoparticles in aquatic and soil environments. PhD. Thesis. ProQuest UMI Dissertation Publishing. 270 pp. ISBN 1249875102.

Vedoucí diplomové práce:	**RNDr. Alena Ševců, Ph.D.** Ústav nových technologií a aplikované informatiky
Konzultant diplomové práce:	**prof. Dr. Kenneth A. Dawson** University College Dublin
Datum zadání diplomové práce:	**21. října 2013**
Termín odevzdání diplomové práce:	**16. května 2014**

prof. Ing. Václav Kopecký, CSc.
děkan

L.S.

prof. Dr. Ing. Jiří Maryška, CSc.
vedoucí ústavu

V Liberci dne 21. října 2013

Prohlášení

Byl jsem seznámen s tím, že na mou diplomovou práci se plně vztahuje zákon č. 121/2000 Sb., o právu autorském, zejména § 60 – školní dílo.

Beru na vědomí, že Technická univerzita v Liberci (TUL) nezasahuje do mých autorských práv užitím mé diplomové práce pro vnitřní potřebu TUL.

Užiji-li diplomovou práci nebo poskytnu-li licenci k jejímu využití, jsem si vědom povinnosti informovat o této skutečnosti TUL; v tomto případě má TUL právo ode mne požadovat úhradu nákladů, které vynaložila na vytvoření díla, až do jejich skutečné výše.

Diplomovou práci jsem vypracoval samostatně s použitím uvedené literatury a na základě konzultací s vedoucím mé diplomové práce a konzultantem.

Současně čestně prohlašuji, že tištěná verze práce se shoduje s elektronickou verzí, vloženou do IS STAG.

Datum:

Podpis:

Acknowledgement

I would like to thank everyone whose support and advice made this thesis possible. This paper would not have been possible without my supervisor, Alena Ševců, and my consultant prof. Kenneth A. Dawson. They have allowed working at two excellent centres, the Instituted for Nanomaterials, Advanced Technology and Innovation (CXI) at Technical University of Liberec (TUL), and the Centre for BioNano Interactions (CBNI) at University College Dublin (UCD). I want to express my gratitude to Nhung A. H. Nguyen and Philip Kelly for help in numerous ways. Especially, Nhung A. H. Nguyen for the toxicity assessment and Philip Kelly for the inspiration. I would like to thank Petr Parma and Hana Pohlreichová for the water chemical analysis, Pavel Kejzlar, Lukáš Voleský and Jana Karpíšková for help with nanoparticle analysis. Finally, the financial support was provided by the project Network for cooperation of academic institution and private sector in the field of environmentally friendly water and soil treatment (CZ.1.07/2.4.00/31.0189) and partly by the project Centre for Nanomaterials, Advanced Technologies and Innovation CZ.1.05/2.1.00/01.0005.

Abstract

Interactions of iron-based nanoparticles with river water and reservoir water were studied in this diploma thesis. NANOFER STAR, Carbo-Iron and ferrihydrite were selected as the representatives of the iron-based nanoparticles. NANOFER STAR is commercially produced for remediation of contaminated soils and ground waters and Carbo-Iron is studied as promising material for advanced application in remediation technologies and thus they would be purposely in contact with the natural environment. Ferrihydrite is a naturally occurring material, here served as a control inert nanoparticle. The study interest was in fate of these nanoparticles in environmentally relevant media. The main objectives were: i) to describe what happens when iron-based nanoparticles are released into aqueous environment; ii) to characterize the nanoparticles using different methods and analyses; iii) to assess potential toxicity of newly prepared and aged nanoparticle suspensions using model bacteria *Escherichia coli*. Real river water samples were obtained from St. Annes Park in Dublin (Irish Republic) and real reservoir water samples were obtained from Harcov reservoir in Liberec (Czech Republic). The nanoparticle suspensions were dispersed in the river water, in the reservoir water and also ultra-pure water and model river water were used. Ultra-pure water was selected as a control dispersive medium without organic matter and other natural compounds and the model RW was created to mimic the river water. The suspensions and nanoparticles were investigated using selected techniques such as Electrophoretic Light Scattering (ELS), Scanning Electron Microscopy (SEM), Energy-Dispersive X-ray Spectroscopy (SEM/EDS), Atomic Force Microscopy (AFM), Brunauer-Emmett-Teller surface area analysis (BET), and the media were characterized based on their pH, Oxidation Reduction Potential (ORP), oxygen concentration, conductivity, temperature, Total Organic Carbon (TOC) and Total Phosphorus (TP). The results in general showed that all particles in the river or the reservoir water increased in diameter over one month. Natural compounds in real environmental media resulted in decrease of electrostatic repulsion and increase in diameter of aggregates. The nanoparticles dispersed in model river water did not behave in a similar way as in natural river water, probably due to lower concentration of TOC and higher conductivity. Moreover, as a consequence of larger size and higher density (about 1 µm and 5 g/ml) of particles, the aggregates and strong sedimentation were observed. Experimental data revealed weakness of the DLS method for dynamic size distribution

analysis of nanoparticles of higher density such as iron. The iron-based nanoparticles were too heavy and unstable in aqueous environment and therefore it was impossible to get reliable data. Nevertheless, DCS is a promising method for iron-based particle analysis. Finally, the toxicity of iron-based nanoparticles tested on *Escherichia coli* was not observed neither in newly prepared nor in aged nanoparticle suspensions.

Keywords: NANOFER STAR, Carbo-Iron, ferrihydrite, nanoparticle characterization, aging of nanoparticles, nanotoxicity, environmental media

Table of Contents

List of Figures

List of Tables

Glossary

Colloid: A homogeneous non-crystalline substance consisting of large molecules or ultramicroscopic particles of one substance dispersed through a second substance. Colloids include gels, sols, and emulsions; the particles do not settle, and cannot be separated out by ordinary filtering or centrifuging like those in a suspension.

Nanocomposite: Denoting a composite material that has a grain size measured in nanometres.

Nanotechnology: The branch of technology that deals with dimensions and tolerances of less than 100 nanometres, especially the manipulation of individual atoms and molecules.

Nanoparticle: A nanoscale particle.

Natural nanoparticles: A nanoscale particle originating from natural processes, e.g. soil colloids.

Engineered nanoparticles: Manufactured nanoparticles.

Size-related intensive properties: Physical or chemical properties of a particle that change as a particle size falls below a certain threshold (surface charge, conductivity, colour, etc.).

Agglomerate: A group of particles held together by relatively weak forces.

Aggregate: A discrete group of particles in which the various individual components are not easily broken apart.

Ultrafine particles: Term frequently used by those dealing with industrial products, aerosols and air pollution, and referring to particulate matter smaller than 2.5 µm.

Abbreviations

AFM	Atomic Force Microscopy
BET	Brunauer-Emmett-Teller surface area analysis
DCS	Differential Centrifugal Sedimentation
DLS	Dynamic Light Scattering
EDS	Energy-Dispersive X-ray Spectroscopy
ELS	Electrophoretic Light Scattering (ELS)
NANOFER STAR*	Wüstite-stabilized nZVI fabricated in April 2013
NANOFER STAR**	Wüstite-stabilized nZVI fabricated in June 2013
ICP OES	Inductively Coupled Plasma – Optical Emission Spectroscopy
ICP MS	Inductively Coupled Plasma Mass Spectroscopy
NP	Nanoparticle
nZVI	nano-sized Zero-Valent Iron
ORP	Oxidation-Reduction Potential
PdI	Polydispersity Index
RW	River Water
SEM	Scanning Electron Microscopy
TOC	Total Organic Carbon
TP	Total Phosphorus
UPW	Ultra-Pure Water
WDS	Wavelength-Dispersive Spectroscopy
HRW	Harcov Reservoir Water

1 Introduction

Natural nanoparticles have existed since life began on Earth. All forms of organisms have been exposed to at least some types of nanoparticles. These organisms have enough time to adapt to this kind of matter. Nevertheless, engineered nanoparticles have been fabricated in huge amount last decade, thus the risk of release of engineered nanoparticles to the environment is evident. What would happen when engineered nanoparticles are exposed to the environment? What are the forces driving transport and fate of nanoparticles? Nanoparticles used in remediation of contaminated soils and ground waters are nanomaterials which are purposely in contact with the natural environment. Iron-based nanoparticles (e.g. NANOFER STAR, Carbo-Iron and ferrihydrite) are promising materials for this application; NANOFER STAR and Carbo-Iron versus ferrihydrite as representatives of engineered and natural nanoparticles, respectively. Are they safe and reliable agent for this kind of application? The effect on the reactivity and stability of the iron-based nanoparticles after at least one-month exposure to river and/or reservoir water was examined and is discussed in this thesis. The behaviour of nanoparticles in the aqueous environments was investigated by Differential Centrifugal Sedimentation (DCS), Dynamic Light Scattering (DLS), Electrophoretic Light Scattering (ELS), Scanning Electron Microscopy (SEM), Energy-Dispersive X-ray Spectroscopy (SEM/EDS), Atom Force Microscopy (AFM), Brunauer-Emmett-Teller surface area analysis (BET), and pH, Oxidation Reduction Potential (ORP), oxygen concentration, conductivity, temperature, Total Organic Carbon (TOC) and Total Phosphorus (TP) measurements.

2 Literature Overview

2.1 Nanomaterials

2.1.1 Definition and Regulation of Nanoparticles

Although a huge amount of engineered nanoparticles is fabricated today, research on safety performed in academia and its incorporation into industrial and regulatory practices are not well-aligned. It is often caused by contradictive published data and studies, in part because of a lack of standardization of protocols and reference materials [1]. Nowadays, it is clear that nanomaterials show a large variety of properties caused by their size, shape, porosity, surface area and chemistry. Nevertheless, some of these parameters became more relevant at smaller scale although not necessarily always. Therefore defining of nanoparticles is not easy task [2], [1].

On 18 October 2011, the European Commission recommended definition of nanomaterial as a natural, incidental or manufactured material containing particles, in an unbound state or as an aggregate or as an agglomerate and where, for 50 % or more of the particles in the number size distribution, one or more external dimensions is in the size range between 1 nm and 100 nm. In specific cases and where warranted by concerns for environment, health, safety or competitiveness the number size distribution threshold of 50 % may be replaced by a threshold between 1 and 50 %. By derogation from the above, fullerenes, graphene flakes and single wall carbon nanotubes with one or more external dimensions below 100 nm should be considered as nanomaterials [3].

Furthermore, it should be mentioned that nanoparticles can be used in final application at different state thus their risk of release into the environment is more or less probable. Commercial applications using nanoparticles fall into three categories (nano-straightened materials, surface-nanostructured materials and bulk-nanostructured materials). In case of nano-straightened materials, nanoparticles are imprisoned in a matrix in order to ensure some new functionality or modify its physical properties such as better resistance to wear of nanocomposites. Surface-nanostructured materials are used to constitute a surface coating. They are more open to the environment than nano-straightened materials but they are still firmly attached to the surface. Conversely, the most open and mobile are bulk-nanostructured materials. These materials are the most risky if the behaviour in the environment is unknown [4].

Nowadays, many organizations at European level try to solve problem with regulations and risks connected to nanomaterials. The most important is the European Chemical Agency (ECHA) with its regulation of chemicals in order to protect human health and the environment, REACH, and communication platform of chemical hazards for workers and consumers, CLP. Next important organization which ensures communication channel in nanomaterials in general is EU NanoSafety Cluster. In addition to cooperation such as in the Organization for Economic Co-operation and Development (OECD) or at UN-level, the EU Commission has started a regular dialogue with the United States in the context of the Transatlantic Economic Council (TEC), with a view to avoiding undesired divergences [1], [5].

2.1.2 Unique Properties of Nanoparticles

Nanoparticles within the size range from 20 nm to 100 nm have very high surface area to volume ratio. Nevertheless, it does not mean that they differ drastically from those of larger size. The reduction of size within this range causes higher influence of interaction between gravity, diffusion and convection forces or other effects connected with high surface area and low weight. They behave as colloids as it is well known. However, there is a critical threshold size below 20-30 nm for which nanoscale effects begin to arise [6]. There are at least two reasons why nanoparticles differ from their larger counterparts in range below 20-30 nm. Firstly, a change in a crystal structure of the particles (e.g., an atomic rearrangement at the surface, presence of crystal defects, appearance of vacancies, and changed morphology) occurs when their size is reduced. Secondly, thermodynamic stabilization of the nanoparticles begins to play key role [6].

Finally, it is necessary to mention that when the particles are small enough they can interact with a matter which is for larger particles unreachable. This matter can unexpectedly interact with important cellular compartments and cause serious changes in their structure, hence function [1]. Nevertheless, the properties of nanoparticles are often related to their final application. The exact composition of the nanoparticles can therefore be split into two or three parts depending on application: a surface that may be functionalized, a shell that may be added and the core. Often nanoparticles are referred only to their core material because that is the part that results in key properties for most applications [7].

2.1.3 Engineered vs Natural Nanoparticles

Natural nanoparticles have been part of environment since a life began on Earth as minerals, clays, and products of bacteria of different compositions and structures (gold, silver, magnetite, maghemite, etc.) [8]. Natural nanoparticles are of central importance in earth system: in global biogeochemical cycles, weathering, metal binding and transport, bioavailability and ecotoxicity [9]. Furthermore, the nanoparticles are used by humans intentionally as finely divided metal colorants for centuries. Therefore organisms have had enough time to adapt to this kind of matter.

However, during the last decade there has been boom in a production of novel engineered nanoparticles which are produced in thousands of tonnes. Their production is increasing exponentially. The world nanotechnology market should weigh in at around 1 000 billion euros per year and it may employ 2 to 3 million people in the world in 2010 to 2015. Products of nanomaterials begin commonly emerging on the market such as part of cosmetics, composites, sensors etc. It is evident that the engineered nanoparticles may be released into the environment. Nowadays, only silver, titanium dioxide, silica, carbon nanotubes and fullerenes are produced in thousands of tonnes but the variety will probably increase soon because of their physicochemical benefits and lower costs. [4], [10]

Engineered nanoparticles share unusual properties as natural nanoparticles but their origin influences their properties. Natural nanoparticles are often covered by hydroxyl groups because water is the most abundant environment, whereas surface of engineered nanoparticles is often coated by synthetic molecules for better properties in final applications. Natural nanoparticles are generally not passivated and they do not have stabilizing or encapsulating ligands bound to their surfaces. They are very abundant (water, air) with low toxicity in general and they can even be highly monodispersed. [11]

2.1.4 Iron-based nanoparticles

This chapter introduces to nanoparticles studied and analysed in this thesis. The nanoparticles can be divided into two groups, engineered and natural nanoparticles. First two (NANOFER STAR and Carbo-Iron) are engineered nanoparticles whereas the NANOFER STAR is commercially available and the Carbo-Iron is an experimental product. Finally, ferrihydrite belongs to natural nanoparticles, although engineered nanoparticles of ferrihydrite were used in this study.

NANOFER STAR is a new product of NANO IRON, Ltd. which is wüstite-stabilized nano-sized Zero-Valent Iron powder (nZVI). The acronym STAR means Surface-stabilized, Transportable, Air-stable and Reactive nZVI. NANOFER STAR contains more than 90 % of ZVI in the core and the rest is of FeO-Fe_3O_4 on the surface shell, which represents stabilizing coating of ZVI nanoparticles. NANOFER STAR keeps high reactivity with reducible pollutants in water environment. The stabilization facilitates manipulation because NANOFER STAR powder can be exposed to air without fast oxidation. This powder is used for direct application as well as for preparation of slurries applied in-situ for groundwater remediation and other applications. [12]

Carbo-Iron is a composite of activated carbon particles (800 µm, D50) anchored by iron clusters. The composite combines the sorption properties of activated carbon and the chemical reactivity of nZVI. The colloids of Carbo-Iron show enhanced mobility in a sediment material compared to standard nZVI even without colloid stabilizers. The chemical nature of particles is hydrophobic thus the particles are accumulated in organic phase where they can easily interact with reagents. The Carbon-Iron nanoparticles have the same application as NANOFER STAR - in-situ groundwater remediation. [13], [14]

Ferrihydrite is a nano-sized metastable hydrated ferric iron mineral ($Fe_2O_3 \cdot 0.5H_20$) which is spread at neutral to slightly acidic conditions. Ferrihydrite has been found in waters, sediments, soils, mine wastes and acidic mine drainage in many locations around the world even inside living organisms as a main component of ferritin core. The ferrihydrite is formed in abiotic conditions primarily by precipitation at low temperature, typically near aerated surfaces. The ferrihydrite formation is often in presence of silica ions which may stabilize and inhibit phase transformations.

Ferrihydrite can be produced in a biological way too, which is performed by iron-oxidizing bacteria and iron-reducing bacteria such as chemolithotrophic *Gallionella* and *Leptothrix* living in many natural systems, including freshwater ferruginous mineral springs, shallow brackish waters, marine hydrothermal shallow water environments, and active, deep sea hydrothermal venting sites, and soil environments. Ferrihydrite is formed by oxidation of dissolved ferrous iron in aqueous solutions and precipitates as an insoluble ferric hydroxide on their stalks or sheaths. These natural nanoparticles represent cheap way for clean-up of polluted soils and waters or they can serve as a precursor for further synthesis due to their relatively high purity and absorption activity for numerous metals such as As and U because of their high surface area. [15], [16]

2.3 Nanoparticles in Aqueous Environment

Many physicochemical approaches for study of colloidal behaviour can help to understand and predict the behaviour of nanoparticles in aquatic environment. Nevertheless, the behaviour of nanoparticles of the same composition may significantly differ in colloidal size range (1 nm to 1,000 nm) because of size-dependent properties. In context of decreasing of the particle size the specific surface area increases. The number of surface atoms to internal atoms begins to increase exponentially when the size of particle is less than 20 nm. The high specific surface area causes very high reactivity connected to decreasing of surface free energy as the Young-Laplace equation describes. [9]

Nanoparticles tend to decrease the free energy of their surface. The possible scenarios depend on the properties of the environment and the nanoparticles. The environment can be characterized based on pH, ionic strength, redox potential, temperature, conductivity and concentration of different type of species (organic and inorganic components of water environment) analysis; and particles are defined based on their size, shape, number, mass, specific surface area, zeta-potential and surface chemistry. The nanoparticles may reorganize themselves into structures with lower free surface energy, aggregate or interact with species in the water environment in respect to previously mentioned parameters. Each process leads to formation of bigger particles which is often followed by sedimentation of these particles. [17]

The atomic rearrangement is the most frequently occurring phenomenon in the natural environment. Nevertheless, the atomic rearrangement is influenced and accompanied by other phenomena strongly depending on wetting of particle surface by water and concentration of present species, especially other colloidal particles or dissolved gases (oxygen). Affinity of nanoparticles to water (polar environment) selects if there is a tendency to agglomeration or to dispersion. Nanoparticles are well dispersed when their surface is hydrophilic and their concentration is low. Other key parameter of colloidal stability is their surface stabilization. It can be electrostatic repulsion or steric hindering. [18]

The electrostatic repulsion is caused by repulsion of surfaces with the same charge. The surface charge is strongly influenced by ionic strength, pH and redox potential of the environment. The ionic strength, pH and redox potential refer to ion neutralization,

protonation or deprotonation strength and oxidation or reduction strength, respectively. Hence, surface chemistry, pH and salinity are the three interdependent parameters determining the affinity of nanoparticles to surrounding particulate matter. The particulate matter can significantly change chemistry of original surface and can cause stabilization or destabilization of nanoparticles. The result depends on the physicochemical parameters of the environment and the nanoparticles surface, and properties of macromolecule (flexibility, dissociation constant, morphology, etc). [9], [19]

Table 2.1. Physicochemical parameters of nanoparticles measured in aquatic environment [17]

	Parameters	Features and Phenomena
Environment	pH	Protonation or deprotonation of chemical groups at the nanoparticle surface
	Redox Potential	Oxidation or reduction of nanoparticle surface
	Ionic Strength (Conductivity)	Neutralization of the nanoparticle surface charge by ions
	Temperature	Higher temperature increases energy of system and number of events per unit of time
	NOM Concentration	Stabilization or destabilization of nanoparticles
	Oxygen Concentration	Higher oxygen concentration facilitates the oxidation of nanoparticle surface
Nanoparticles	Size and Shape	Reactivity of nanoparticle
	Number and Mass	Weight of nanoparticle
	Specific Surface Area	Surface capacity for reactions
	Zeta-Potential	Colloidal stability
	Surface Chemistry	Surface reactivity

2.4 Methods for Nanoparticle Characterization

2.4.1 Nanoparticle Characterization

Determination of physical and chemical properties of nanomaterials is addressed to novel subfield of metrology, nanometrology. The challenge of nanometrology is to develop new measurement techniques and standards for nanotechnology. The most important nanoparticle parameters are size, concentration, agglomeration/aggregation, shape, surface area, surface charge and mass. The methods characterizing these parameters are listed in the following table. [20]

Table 2.2. Devices and methods for nanoparticle characterization [20]: commonly used for this type measurements (●), can be used with some limitation (○).

	Size	Number Concentration	Agglomeration / Aggregation	Shape	Surface Area	Surface Charge	Mass
Atomic Force Microscopy	●			○			
Electron Microscopy	●		○	●			
Optical Microscopy	●		○	●			
Dynamic Light Scattering	●		○				
Partial Track Analysis	●	●	●			●	
Static Light Scattering: Laser Diffraction	●		●	○			
Differential Centrifugal Sedimentation	●	○	●				
Gravitational Sedimentation	●		●				
Micro Channel Resonator	●	○					●

	Size	Number Concentration	Agglomeration / Aggregation	Shape	Surface Area	Surface Charge	Mass
Electrical Zone Sensing	●	●	○				
Optical Particle Counter	●	●	●	●			
Field Flow Fractionation	●		○				
Gas Adsorption			○		●		
Streaming Current / Potential						●	
Electrophoretic Light Scattering						●	
Microseaving	○		○				
Thermogravimetric Analysis							●

Analytical methods and devices used in this study are described in more details in the following chapters (2.4.2 – 2.4.6), the principle of: Atomic Force Microscopy (AFM), Scanning Electron Microscopy (SEM), Differential Centrifugal Sedimentation (DCS), Dynamic Light Scattering (DLS) and Electrophoretic Light Scattering (ELS).

2.4.2 Atomic Force Microscopy

Atomic Force Microscopy (AFM) is a type of scanning probe microscopy developed to investigate non-conductive surfaces with high resolution, up to 1 MX. Obtained image gives, unlike electron microscopy, three-dimensional information about the surface, because AFM uses a very sharp tip (usually 10 nm in diameter) and measures its position in three dimensions. Next advantage of AFM is that it can operate even under atmospheric pressure and different environments like atmosphere or even aqueous solutions. AFM can operate in different modes based on the distance between the sample and the tip (Fig. 2.1). The difference occurs in the force direction affecting the tip as a result of interaction between the tip and the sample. The interpretation of AFM images can be difficult because the image can show different kinds of artefacts related to the shape and material of the tip (Fig. 2.2). [21]

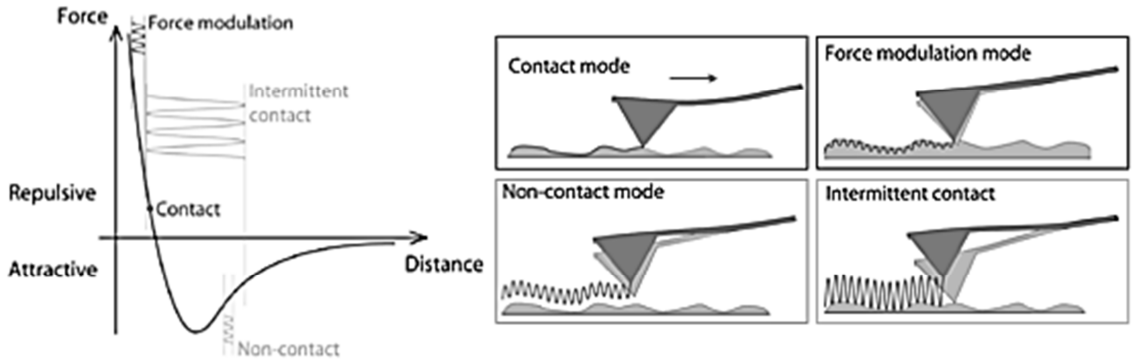

Figure 2.1. AFM modes: Different AFM modes related to the graph of force as function of distance between a sample and a tip. [22]

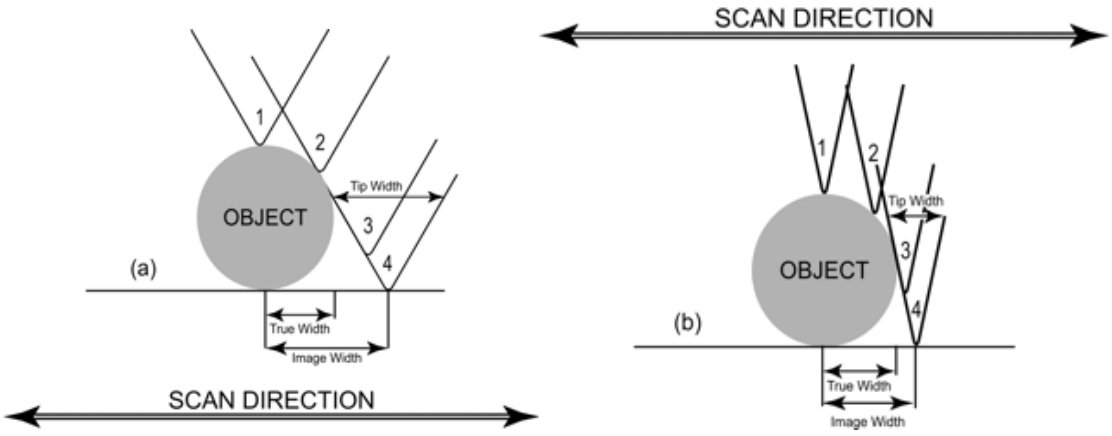

Figure 2.2. Accuracy of AFM tip: blunt tip (a); sharp tip(b). [23]

2.4.3 Electron Microscopy

There are two important types of electron microscopy, Transmission Electron Microscopy (TEM) and Scanning Electron Microscopy (SEM). Nevertheless, SEM was used for the nanoparticle analysis at TUL. They differ in process of obtaining information about a sample: SEM from the same side and TEM from opposite side of incident electron beam. Therefore, sample preparation requirements for TEM comparing to SEM are much higher, for example a sample for TEM analysis must be very thin. Electron microscopy works with electron beam thus a sample is analysed in vacuum and has to be dry. Next complication is charging of unconductive samples. The samples are either placed on a conductive target or coated by thin layer of gold or the operation voltage has to be decreased (lower energy of an incident beam). The principle of SEM analysis of surface topology is shown in the following figure 2.3. The information is obtained from the intensity of secondary electrons emitted after collision of the electron beam with a region at the surface of the sample. The secondary electrons originate from the surface itself and the region under the surface as well. The image of TEM and SEM do not give direct information about depth or height but the magnification can be very high (up to 50 MX for TEM and up to 2 MX for SEM). [24]

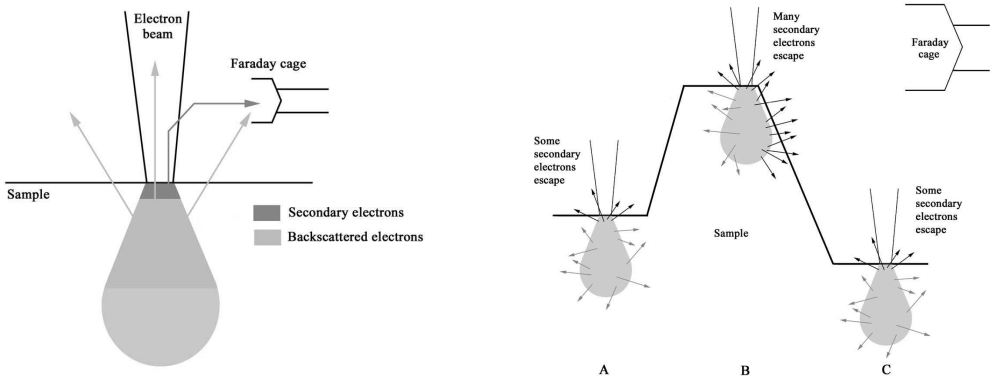

Figure 2.3. Principle of SEM: Interaction volume between electron beam and specimen (left); edge effect, signal from edges and peaks is much higher than from valleys (right). [25]

2.4.4 Differential Centrifugal Sedimentation

The Differential Centrifugal Sedimentation (DCS) is actually a rate-zonal centrifugation. The sample is placed on top of a density gradient where centrifugal force begins to act (Fig. 2.4). The sample usually contains particles of different size but same density. Bigger particles move faster than smaller. It means that particles are sorted by size, approaching a detector at different time. This way the particle size distribution is created. [26], [27]

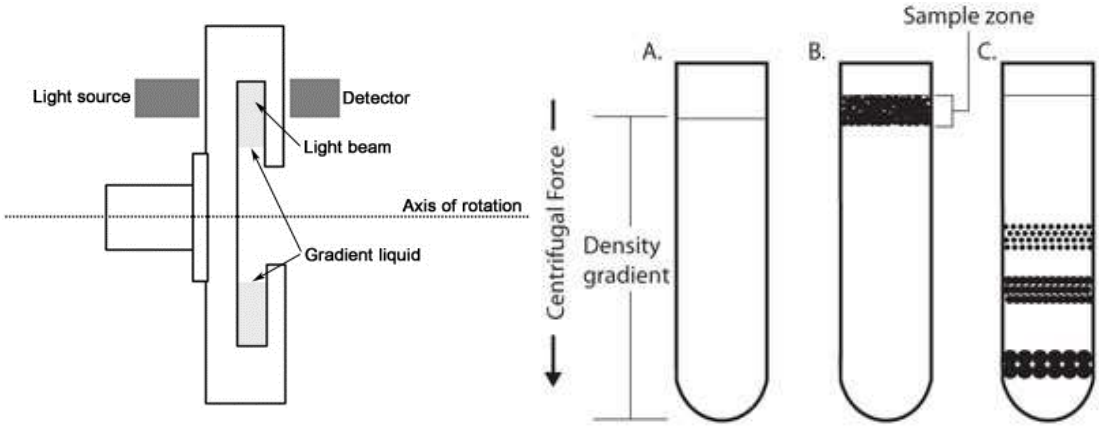

Figure 2.4. Principle of DCS: Cross section view of Disk Centrifuge (left) [28]; Principle of Rate-Zonal Centrifugation (right) [27].

2.4.5 Dynamic Light Scattering

Dynamic Light Scattering (DSL) is a non-invasive technique allowing to measure particle size distribution typically in the submicron regime in suspensions. The method is based on laser light scattering over time where smaller particle scatter light more randomly than larger ones because Brownian motion of smaller particles is more significant (Fig. 2.5). Particle size is obtained when dynamic information about intensity is evaluated by the time-correlation functions and Stokes-Einstein equation. [29]

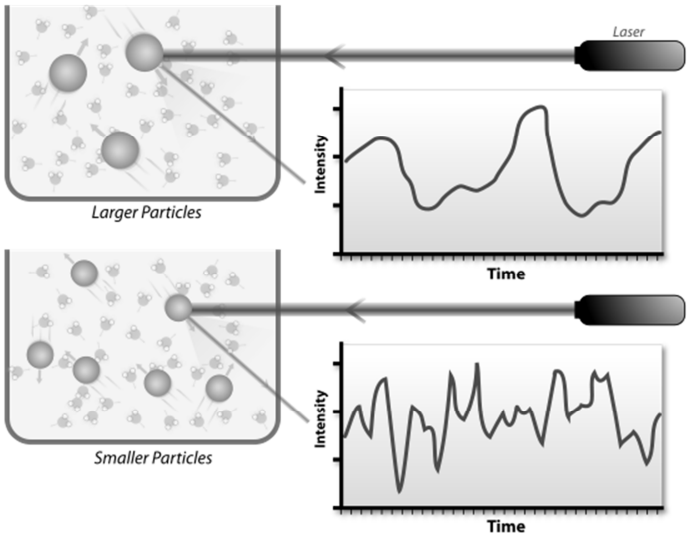

Figure 2.5. Principle of DLS: Hypothetical dynamic light scattering of two samples, larger particles on the top and smaller particles on the bottom. [29]

2.4.6 Electrophoretic Light Scattering

Electrophoretic Light Scattering (ELS) is a technique for detection of zeta-potential. Therefore it refers to colloidal stability. The technique is based on measuring of particle velocity in electric field by a combination of Doppler velocimetry and phase analysis of light scattering. Zeta-potential provides information about the potential at outer part of slipping plane with respect to surrounding environment (0 V) (Fig. 2.6). The region of instability is generally considered between +30 or -30 mV. [30]

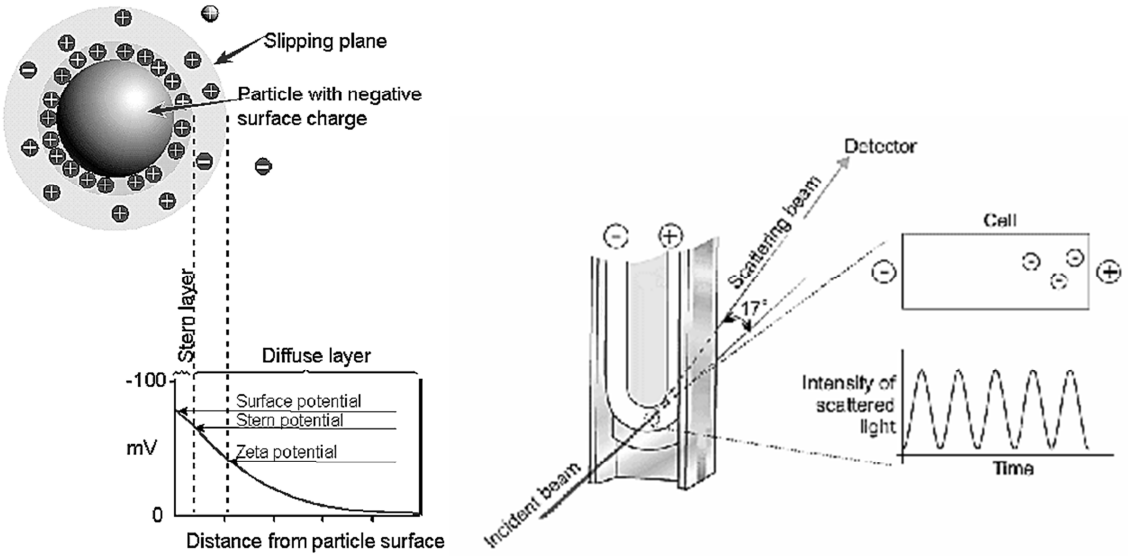

Figure 2.6. Zeta-potential: Physical meaning (left); Experimental determination of zeta-potential (right). [31]

2.5 Methods for Environmental Media Characterization

The intrinsic properties of nanoparticles, notably their surface properties, are determined by the surrounding environment. The list of parameters and analysis methods of nanoparticles were listed in Chapter 2.3. The methods and their probes or detectors for environmental media characterization, which were used in this work, are listed in Tab. 2.3. Most of these methods are based on electrometric measurements by two electrodes, reference electrode and measuring electrode. The material and the construction of electrodes determine their use.

Table 2.3. Environment parameters and their methods [32][33]

	Method	**Probe / Detector**
pH	Electrometric measurement	Ag/AgCl reference electrode Glass electrode
Oxidation Reduction Potential (ORP, mV)	Electrometric measurement	Hydrogen reference electrode Platinum electrode
Concentration of Dissolved Oxygen ([O2], mg/l)	Electrometric measurement	Ag/AgCl reference electrode Membrane electrode
Concentration of Natural Organic Matter ([NOM], mg/l)	Thermocatalytic oxidation, Total Organic Carbon TOC	Multi-channel non/dispersive infrared detector (MC/NDIR)
Conductivity (κ, µS/cm)	Electrometric measurement	Metal electrodes
Temperature (T, °C)	Fluid-expansion measurement	Glass bulb with fluid

2.5 Ecotoxicity of Nanoparticles

Engineered nanoparticles bring important innovations in technology, medicine, energy harvesting materials, because of their unique properties (see Chapter 2.1). Problem might arise when nanoparticles are released into the environment. They can be either harmless or very toxic to humans and other organisms. The risk assessment has been in progress, lead by international organizations such as the European Chemical Agency (ECHA) and OECD. However, the existing EU legislative regulations do not include unique properties of nanoparticles, so they are currently treated as other chemicals. Nevertheless, the description of risk and properties of nanoparticles is a very difficult task, because nanoparticles vary too much and one regulation cannot cover all consequences. Still, at least several paradigms can be discerned according to recent toxicity studies [34]:

- The importance of nanoparticle localization which will determine organs or functions potentially affected
- The importance of intrinsic nanoparticle reactivity, and in particular redox activity
- Nanoparticle-induced oxidative stress seems to be common in many organisms
- The importance of toxicity and solubility of the chemical elements, e.g., Cd, Zn that form nanoparticles

3 Materials and Methods

3.1 Iron-Based Nanoparticles

3.1.1 NANOFER STAR

NANOFER STAR is a new product of NANO IRON, Ltd. which is wüstite-stabilized nano-sized Zero-Valent Iron powder (nZVI). The acronym STAR means Surface-stabilized, Transportable, Air-stable and Reactive nZVI. NANOFER STAR contains more than 90 % of ZVI in the core and the rest is of FeO-Fe_3O_4 on the surface shell (Fig. 3.1a), which represents stabilizing coating of ZVI nanoparticles (Fig. 3.1b). [12]

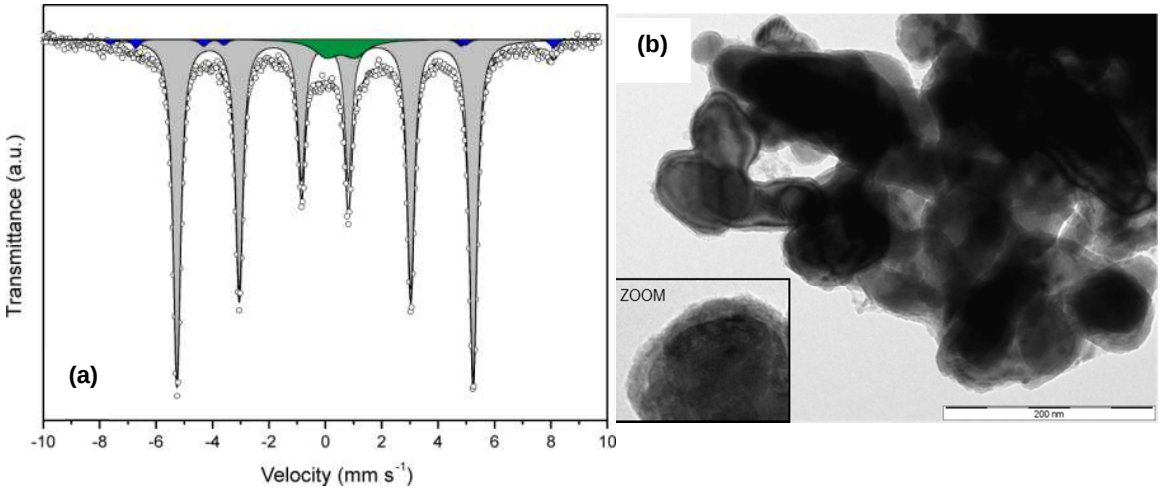

Figure 3.1. Mossbauer spectrum and morphology of NANOFER STAR: Mossbauer spectrum: nZVI – grey spectrum, Fe_3O_4 – blue spectrum, FeO – green spectrum (a); TEM image of nanoparticles covered by visible oxidic shell (b). [35]

3.1.2 Carbo-Iron

Carbo-Iron was obtained from Helmholz Centre for Environmental Research, Germany. Carbo-Iron is a composite of activated carbon particles (800 µm, D50) anchored by iron clusters (Fig. 3.2). [13], [14]

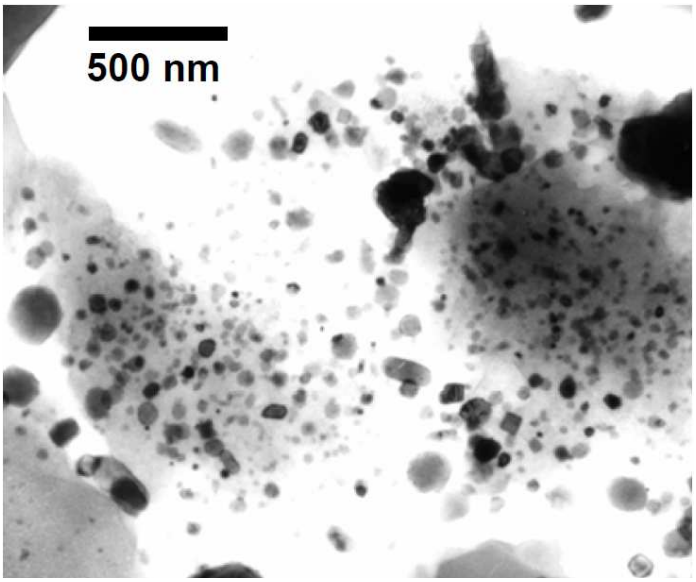

Figure 3.2. TEM image of Carbo-Iron: Bright-field image of iron particles on carbon grains with 20 wt-% nZVI. [13]

3.1.3 Ferrihydrite

Ferrihydrite (Fig. 3.3) was obtained from Palacky University, Olomouc, Czech Republic. Ferrihydrite is a nano-sized metastable hydrated ferric iron mineral ($Fe_2O_3 \cdot 0.5H_20$) which is spread at neutral to slightly acidic conditions. [15], [16]

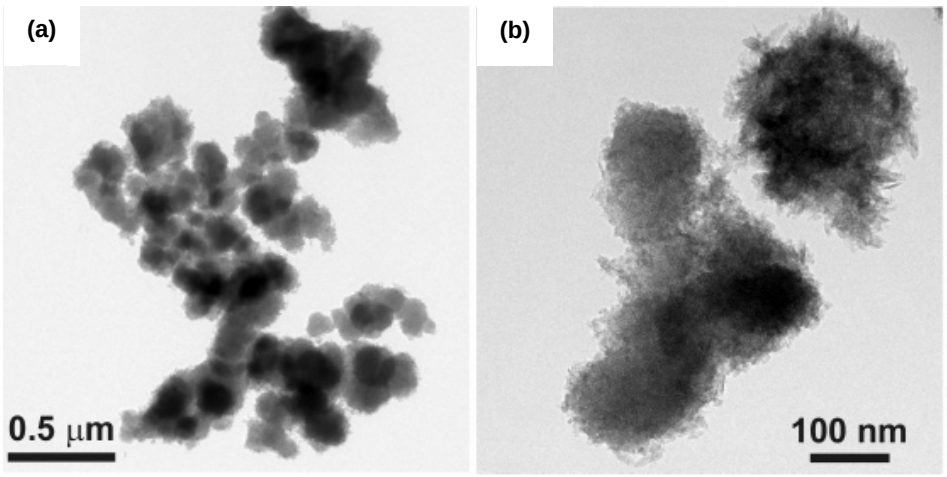

Figure 3.3. TEM images of ferrihydrite: Ferrihydrite aggregates (a); Detail of ferrihydrite aggregates rimmed by acicular crystals of goethite (b). [16]

3.2 Environmental Media

3.2.1 Media Used in Experiment at UCD

The River Water (RW) was collected into a PET bottle (1.5 l) from the river in Saint Anne's Park in Dublin (53° 22' 19.3'' N, 6° 10' 22.5'') on 11th of July 2013. The RW was not filtered, just transferred into a glass bottle with a plastic cap and stored in a fridge.

A model River Water (model RW) was prepared as a simple model of RW from Saint Anne's Park in Dublin. The model RW mimicked pH, conductivity and organic components by adding phosphate buffer, sodium chloride and humic acid into ultra-pure water. The model RW had pH 8.2, 550 µS/cm and contained 5 mg/ml humic acid. The concentration of humic acid was estimated from solid phase by evaporating of RW at 60 °C in a vacuum centrifuge for vials (Concentrator plus). The model RW was stored in a glass bottle with cap in a fridge. The control media was Ultra-Pure Water (UPW).

The media with increased fraction of nitrogen were created from RW, model RW and UPW (RW+N_2, model RW+N_2, UPW+N_2). They were made by nitrogen blowing from disposable glass pipette into glass flask with the medium for 10 minutes before use.

3.2.2 Media Used in Experiment at TUL

The Harcov Resevoir Water (HRW) was collected into PET bottles (3 l) from surface close to the coast of the reservoir in Liberec (50° 46' 16.3'' N, 15° 04' 36.8'' E, 380 m a. s. l.) on the 3rd of March 2014 (Fig. A2). The HRW was filtered over 0.22 µm membrane filter into a glass flask to remove bacteria and stored in a fridge. The control media was Ultra-Pure Water (UPW).

3.2.3 Total Organic Carbon and Total Phosphorus

The Total Organic Carbon (TOC) of unfiltered RW and model RW was measured directly without dilution by the external laboratory. TOC and Total Phosphorus (TP) were measured in filtered HRW (Chapter 3.2). TOC in HRW was measured directly using MULTI N/C (Analytic Jena, Germany). The sample of HRW for TP was acidified by HNO_3 and measured using ICP OES (OPTIMA 2100DV, Perkin Elmer). The sample of HRW was diluted ten times and the measuring was repeated using ICP MS (NexIon 300D, Perkin Elmer) with higher sensitivity (< 0.002 mg/l).

3.3 Suspensions of Iron-Based Nanoparticles in Environmental Media

3.3.1 Experiment at UCD

Stock suspensions of nanoparticles (NANOFER STAR*, NANOFER STAR**; Chapter 3.1) were prepared in six different media (RW, RW+N_2, model RW, model RW+N_2, UPW, UPW+N_2; Chapter 3.2) Nanoparticles were stored in powder state in Falcone tubes before use. First, the powder was weighed on the precise balance in a new 50 ml Falcone tube in a fume hood. After that, the medium was added into the Falcone tube to create 10 g/l of stock suspension. The stock suspension was vortexed at the highest speed for one minute and then it was homogenized in ultrasonic bath for one minute. Subsequently, 50 mg/l, 250 mg/l and 500 mg/l suspensions were prepared from the stock suspension by diluting it by the relevant media in 15 ml Falcone tube (medium) or 1.5 ml vial (medium+N_2) and closed. The suspensions were stored about one month at laboratory conditions before further characterization (Fig. A1). The samples in vials (NPs + medium + N_2) were stored and opened only once, right before the analysis.

3.3.2 Experiment at TUL

Stock suspensions of three different nanoparticles (NANOFER STAR*, ferrihydrite, Carbon-Iron; Chapter 3.1) were prepared in fresh Ultra-Pure Water (UPW). Iron-based nanoparticles were stored in powder state in Falcone tubes before use. Each sample of nanoparticles was transferred into a new 50 ml Falcone tube in a fume hood and then weighed in a range of 250 – 260 mg on a precise analytical balance. Next step was to add UPW to prepare 5 g/l of stock suspension. The suspensions were homogenized using table vortex and stored in a fridge (4 – 8 °C) for two days. After that, each suspension was divided into two Falcone tubes and homogenized by high speed homogenizer (MICCRA D-9, DS-8/P dispersing tool, ART Prozess- & Labortechnique, Germany) for one minute at 39,000 rpm. Finally, each suspension was vortexed at the highest speed.

Tested suspensions were prepared few minutes after the final homogenization of the stock suspensions. The final suspensions were prepared from fresh HRW (Chapter 3.2) and fresh UPW. The suspensions were prepared in two concentrations (50 and 500 mg/l) for each stock suspensions of nanoparticles (NANOFER STAR*, ferrihydrite, Carbon-Iron). First, 198 ml or 180 ml of the dispersant (UPW and HRW, respectively)

was added into 1-L sterilized Erlenmeyer flask. Then an adequate amount of stock suspension (2 or 20 ml) was added to create 200 ml of suspension. Finally the flasks were sealed by an aluminium foil and put on a table in front of a laboratory window (Fig. A3).

3.4 Characterization of Pristine and Aged Nanoparticles

3.4.1 Specific Surface Area and Chemical Composition

The nanoparticles (NANOFER STAR*, Carbo-Iron and ferrihydrite) were transferred directly into the measuring cell of the instrument (Autosorb IQ-MP, Quantachrome Instruments, USA) without any modification. The samples were degassed in a vacuum at 105 °C for 12 hours. The specific surface area was determined by a standard procedure of multipoint BET method (5 points, $p/p_0 = 0.1 – 0.3$).

The powders of nanoparticles (NANOFER STAR*, Carbo-Iron and ferrihydrite) were analysed by Scanning Electron Microscopy with Energy-Dispersive X-ray Spectroscopy (SEM/EDS; Carl Zeiss ULTRA PLUS/OXFORD INSTRUMENTS, Germany/United Kingdom) to determine elemental composition. The characterization was made without any treatments of the samples. The powders were directly transferred onto a sticky carbon foil of the target.

3.4.2 Morphology

The SEM analysis of powder nanoparticles (NANOFER STAR*, Carbo-Iron and ferrihydrite) and aged particles obtained from suspensions prepared at TUL (500 mg/l – UPW/HRW – NANOFER STAR*/ Carbo-Iron/ ferrihydrite) was performed by UHR FE-SEM (Carl Zeiss ULTRA PLUS, Germany) using the In-Lens SE detector.

The characterization of nanoparticle powders was performed at 25 KX and 50 KX magnifications under 1.5 kV without any treatments of the samples. The powders were directly transferred onto a sticky carbon foil of the target. The size distribution of nanoparticles was made in ImageJ software (National Institute of Health, USA; http://imagej.nih.gov/ij/).

Each sample of aged nanoparticles was prepared by pipetting 50 µl of HRW or UPW suspension on the sticky carbon foil of target in a laminar flow box where the drops of suspensions were dried over 2 days. The dried samples were directly measured at 50 KX and 100 KX magnification under 2.5 kV without any further treatments. The size distribution of nanoparticles was made in ImageJ software.

The AFM analysis of aged nanoparticles from suspensions (500 mg/l – UPW/HRW – NANOFER STAR*/ Carbo-Iron/ ferrihydrite/) was performed using AFM (JPK

Nanowizard III, Germany) in non-contact mode. The nanoparticle samples were prepared by pipetting of suspension drops onto one microscope slide in laminar flow box and let dried there for two days. The slide with nanoparticle samples was measured after 2 weeks without any further treatments.

3.4.3 Particle Size Distribution

The nanoparticle suspensions from the experiment at UCD and TUL were subjected to Differential Centrifugal Sedimentation (DCS) measurement (DC24000 Disc Centrifuge, CPS Instruments, UK). First, the disk was set at constant speed (5,000 rpm for 0.1 – 2.5 µm and 18,000 rpm for 0.1 – 1 µm) and the sucrose gradient (8 % – 24 %, 9 times 1.6 ml + 0.5 ml dodecane) was built. A calibration standard was injected (0.1 ml of PVC with peak at 0.476 µm) before each injection of the nanoparticle suspension. The values 0.5, 1.7 and 5.24 g/ml were set in CPS software as particle parameters for absorption, refractive index and density, respectively. Each sample was vortexed in 15 ml Falcone tube at highest speed for 30 s before injection (0.1 ml).

The samples from the experiment at UCD and TUL were subjected to Dynamic Light Scattering (DLS) measurement by Zetasizer (NANO ZS, Malvern Instruments, UK). First, the procedure was created with values 1.7, 0.5 for refractive index and absorption for material, respectively, and 25 °C, 0.8872 cP, 1.33 for temperature, viscosity and refractive index for medium, respectively. The detection angle at 173° and analysis model for general purpose was set. Before each measuring, the sample (15 ml Falcon tube or 1.5 ml vial) was vortexed at the highest speed for 30 s, injected into low volume disposable sizing cuvette (ZEN0112) and warmed up to 25 °C for 2 minutes.

3.4.4 Physico-chemical Parameters

Zeta potential of nanoparticle suspensions from UCD experiment (Chapter 3.3.2) was measured using Zetasizer (NANO ZS, Malvern, UK). First, the procedure was created with values 1.7, 0.5 for refractive index and absorption for material, respectively, and 25 °C, 0.8872 cP, 1.33 for temperature, viscosity and refractive index for medium, respectively. Before each measurement, the sample (15 ml Falcone tube or 1.5 ml vial) was vortexed at the highest speed for 30 s, transferred into disposable sizing cuvette (DTS0012) and warmed up to 25 °C for 2 minutes.

The nanoparticle suspensions from TUL experiment (Chapter 3.3.2) were subjected to measurement of pH, ORP, conductivity and temperature. Furthermore, the concentration of dissolved oxygen in HRW and UPW was measured. The multimeter (Multi 340i, WTW, Germany) with probes pH/temperature (SenTix 41, WTW, Germany), ORP (SenTix ORP, WTW, Germany), conductivity (TetraCon 325, WTW, Germany) was used and multimeter Multi 350i, WTW with oxygen probe (OxiCal-CX, WTW, Germany) was used. All measurements were made in a laminar flow box. ORP, pH and oxygen concentrations were very unstable therefore 5 values were recorded during the first minute. Conversely, conductivity and temperature were stable therefore one value was recorded.

4 Results and Discussions

4.1 Properties of Initial Nanoparticle Powders

The nanoparticle powder (nanopowder) of NANOFER STAR*, Carbo-Iron and ferrihydrite was investigated by Scanning Electron Microscopy (SEM) to determine the morphology and size-distribution of nanoparticles, by SEM with Energy-Dispersive X-ray Spectroscopy (SEM/EDS) to determine elemental composition, and by Brunauer-Emmett-Teller surface area analysis (BET) to determine specific surface area of nanoparticles.

The analysis of nanoparticle size in powder state was difficult task because the single nanoparticles were uneasy to distinguish from each other because they form aggregates. The aggregates were often larger than one micron. Nevertheless, the particles stick together because of Van der Waals interactions. However, the aggregates could be broken down either into smaller aggregates or into even single nanoparticles by external forces (see Chapter 4.2). The solution was to measure the nanoparticle size manually (Figs. A6, A8, A10). All measured powders were formed by nanoparticles based on the definition of nanomaterial by European Commission (Chapter 2.1.1). They had at least one dimension bellow 100 nm. Tab. 4.1 shows that the largest specific surface area had nanopowder of the NANOFER STAR* (17.2 m^2/g) and the smallest specific surface area had the nanopowder of the Carbo-Iron (12.3 m^2/g). The specific surface area corresponds to the average diameter of nanoparticle, the largest surface area was formed by smallest nanoparticles and conversely.

Table 4.1. Properties of nanopowders (NANOFER STAR*, ferrihydrite, and Carbo-Iron): specific surface area, average diameter and elemental composition.

Nanopowder	Specific Surface Area (m^2/g)	Diameter (nm)	Elemental Composition
NANOFER STAR*	17.2	46 ± 13	Fe, O
Ferrihydrite	13.4	100 ± 30	Fe, O
Carbo-Iron	12.3	110 ± 100	Fe, C

The SEM images showed that morphology of NANOFER STAR* powder and ferrihydrite is very similar (Figs. 4.1 and 4.2). There is difference in particle size only; nanoparticles of NANOFER STAR* (Fig. 4.1) are larger than nanoparticles of

ferrihydrite (Fig 4.2). The Carbo-Iron nanopowder looked different (Fig. 4.3). The nanopowder was formed by bigger carbon particles and smaller iron particles (see Chapter 3.1.2) similar to particles of NANOFER STAR* or ferrihydrite. The data on their size distributions determined from SEM images are in the appendix (Figs. A5 – A10).

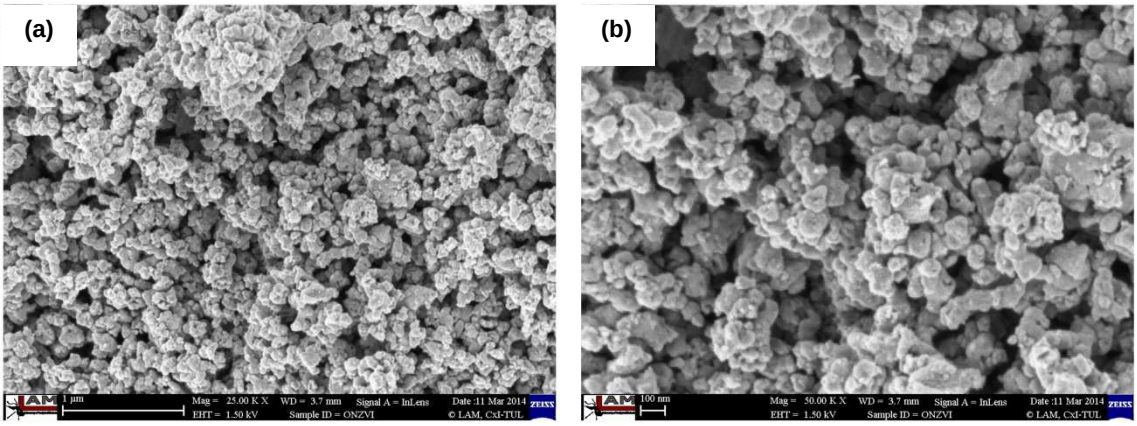

Figure 4.1. SEM images of NANOFER STAR* powder: 25 KX (a); 50 KX (b) magnifications.

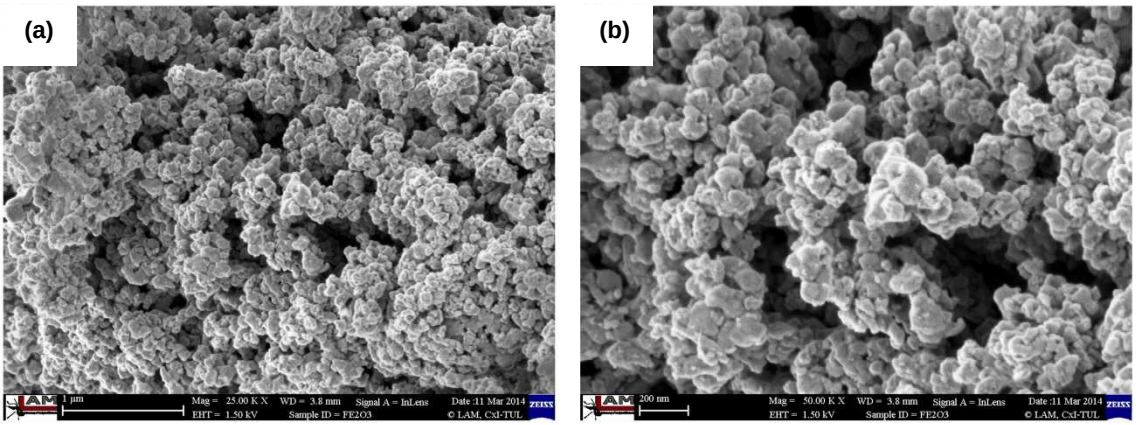

Figure 4.2. SEM images of ferrihydrite powder: 25 KX (a); 50 KX (b) magnifications.

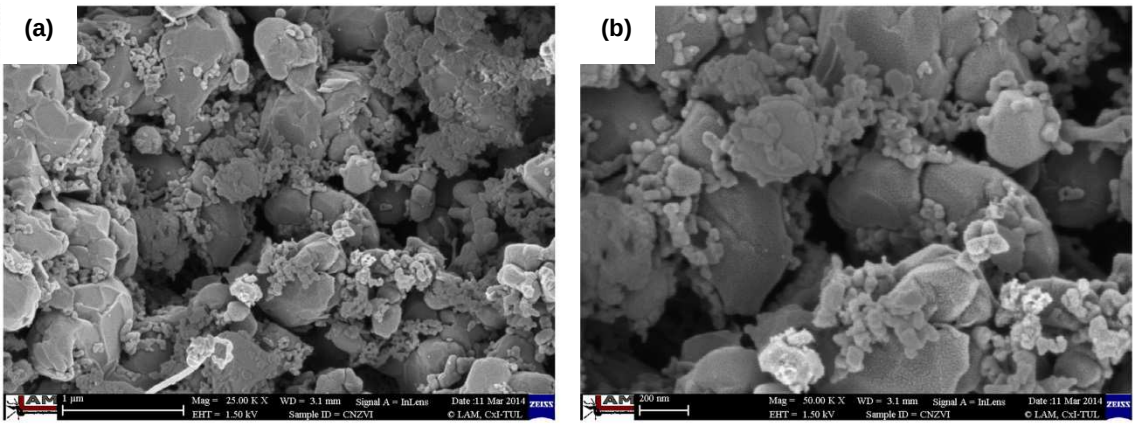

Figure 4.3. SEM images of Carbo-Iron powder: 25 KX (a); 50 KX (b) magnifications.

Although the Carbo-Iron powder was analysed by SEM/EDS, the carbon nanoparticles were not possible to recognize from iron nanoparticles. It was caused by too large interaction region (about 1 µm). Nevertheless, there were found visible differences in elemental composition of nanoparticles. All nanopowders were formed by iron but oxygen and carbon were present in different amounts (Figs. A23 – A25). The oxygen was the most abundant in the ferrihydrite powder and the rarest in the Carbo-Iron powder. The carbon was conversely the most abundant in the Carbo-Iron powder and the rarest in the NANOFER STAR* (Figs. 4.4 – 4.6).

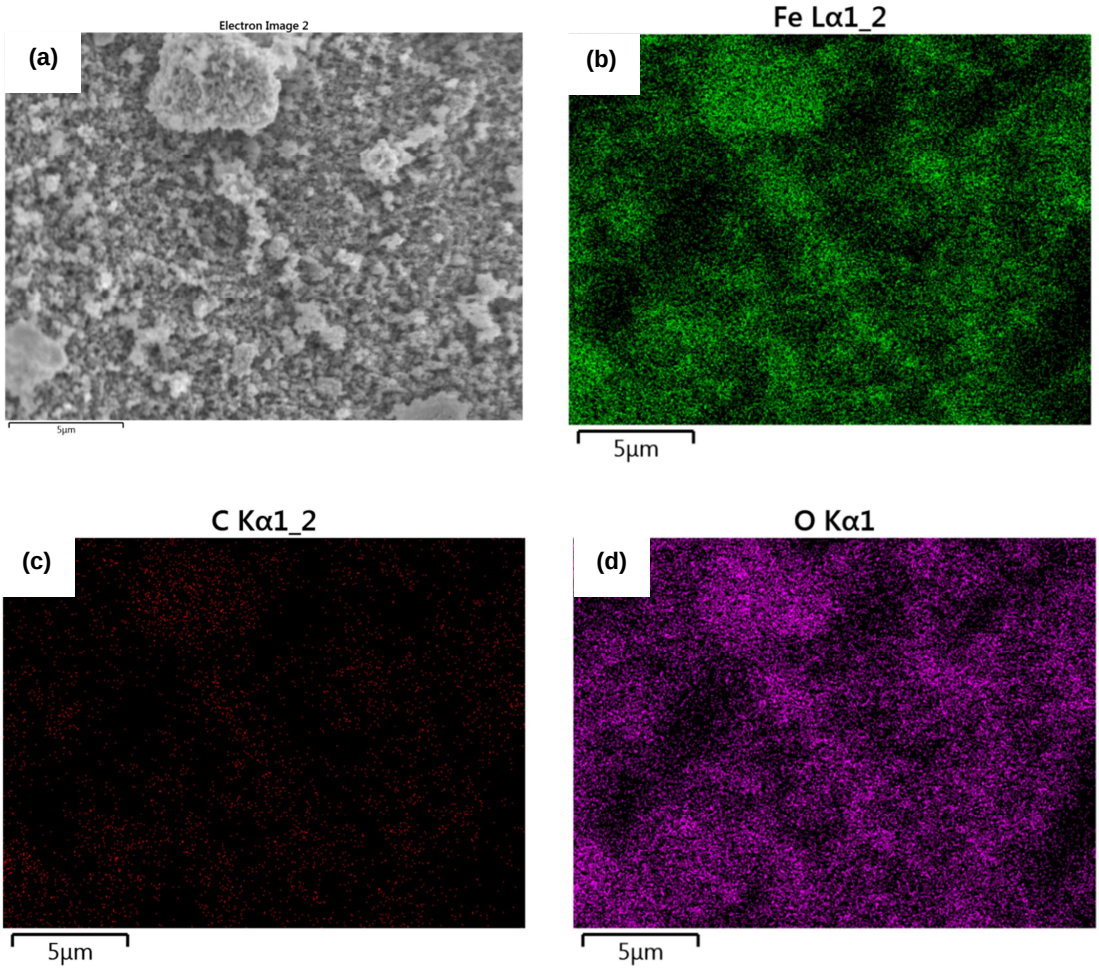

Figure 4.4. EDS mapping of NANOFER STAR* powder: SEM image (a); EDS signal from Fe Lα1_2 (b); EDS signal from C Kα1_2 (c); EDS signal from O Kα1 (d).

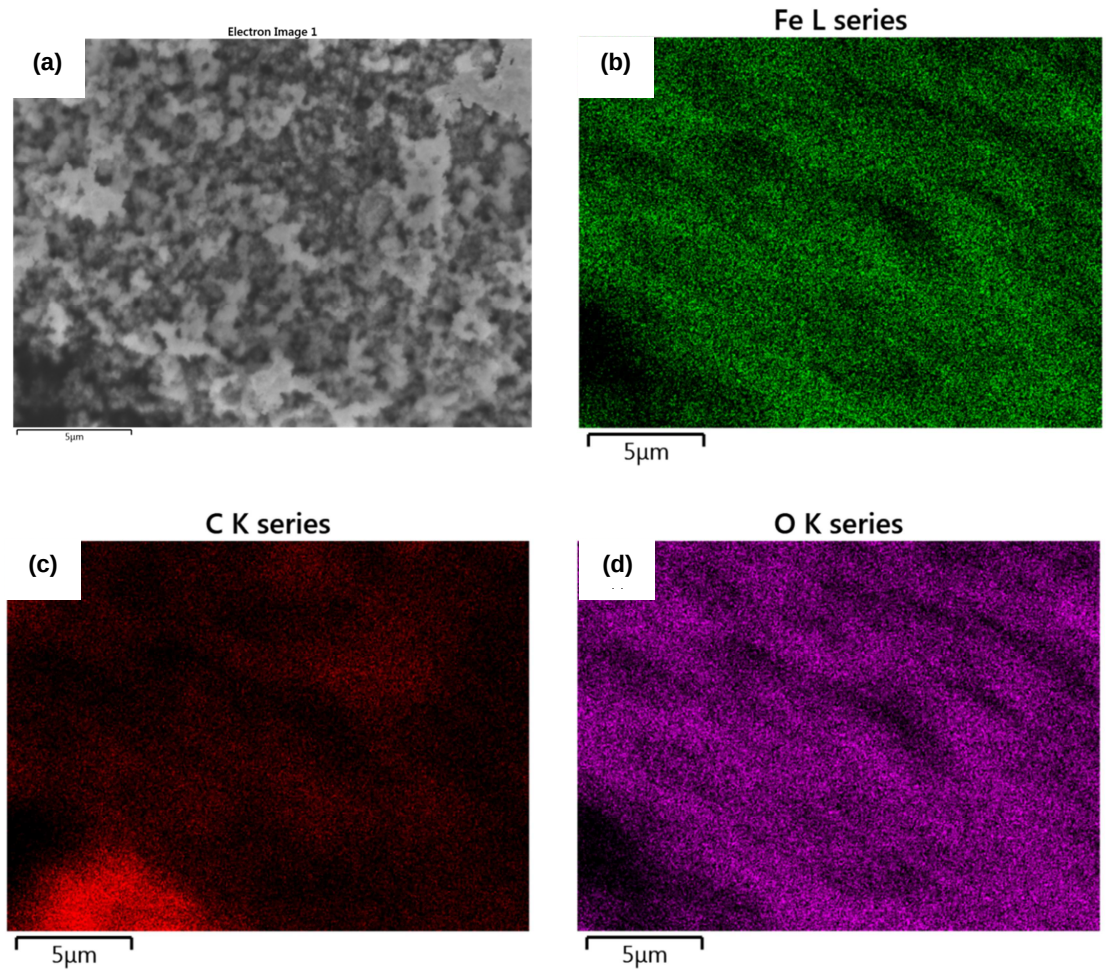

Figure 4.5. EDS mapping of ferrihydrite powder: SEM image (a); EDS signal from Fe L series (b); EDS signal from C K series (c); EDS signal from O K series (d).

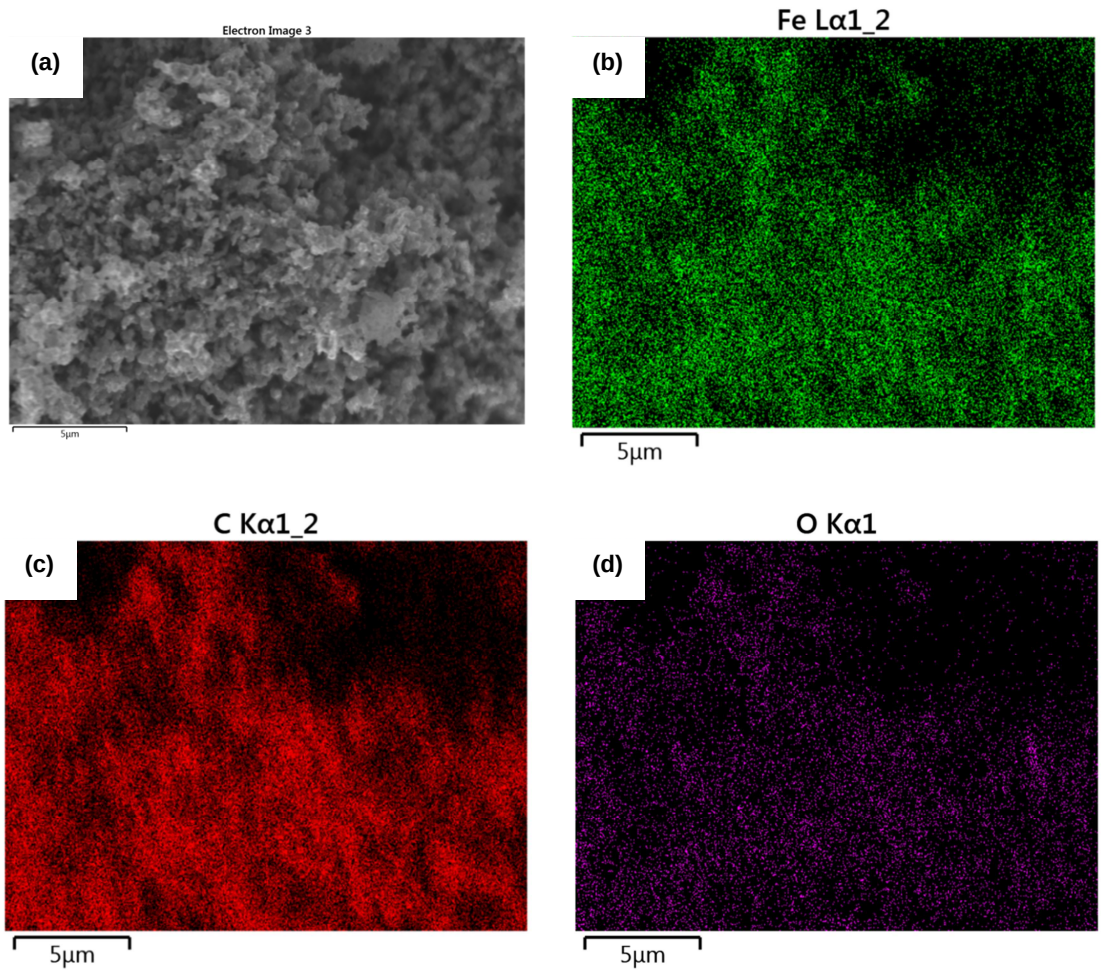

Figure 4.6. EDS mapping of Carbo-Iron powder: SEM image (a); EDS signal from Fe Lα1_2 (b); EDS signal from C Kα1_2 (c); EDS signal from O Kα1 (d).

4.2 Suspensions of Nanoparticles in Environmental Media

4.2.1 Characterization of Suspensions – Experiment at UCD

The dispersive media (RW, model RW, UPW) for NANOFER STAR (*/**) and ferrihydrite suspensions were characterised over a time period. Temperature, pH and conductivity were measured at the beginning and after 35 days in RW (Tab. 4.2). Model RW was measured only at the beginning because there was not sufficient volume after 35 days. The conductivity of RW corresponds to freshwater streams (100 – 2,000 µS/cm) not seawater (5,500 µS/cm) or industrial wastewater (10,000 µS/cm) [36], although the river was close to a seacoast.

Table 4.2. RW, model RW and UPW parameters (pH, temperature, conductivity and TOC), estimated values (*)

Medium / Time (days)		pH	Temperature (°C)	Conductivity (µS/cm)	TOC (mg/l)
RW	0	8.15 ± 0.03	22.1 ± 0.6	391 ± 4	2.59 ± 0.07
	35	8.52 ± 0.02	22.4 ± 0.9	327 ± 4	
Model RW	0	8.2	23	550	0.86 ± 0.02
	35				
UPW	0	7*	25*	0.5 – 3.0*	0*
	35				

The suspensions of NANOFER STAR (*/**) and ferrihydrite were created by mixing the nanoparticles in RW, model RW and UPW (final concentration was 250 mg/l) two times. First was let aged for one month and second was created after 14 days of preparation of the "aging" suspensions. The "aging" suspensions were analysed at the beginning and after 29 days using DCS. The hydrodynamic size of nanoparticle aggregates was increasing over the time in all types of media and for all types of nanoparticles. All types of nanoparticles in RW showed the same properties comparing to nanoparticles in UPW. They were distributed into two populations while all types of nanoparticles in UPW just created slightly larger aggregates and no division into populations was observed (Tab. 4.3, Figs. 4.7 – 4.9).

Table 4.3. DCS hydrodynamic diameter of "aging" suspensions: NANOFER STAR (*/) and ferrihydrite in UPW and RW (250 mg/l) at the beginning and after 29 days; WM (Weight Mean by diameter); NM (Number Mean by diameter); Peak (weight Peak diameter); $w_{1/2}$ (width of weight peak diameter at 0.5 its size).**

NP	Medium / Days		hydrodynamic diameter (nm)					
			WM1	NM1	Peak1	$w_{1/2}1$	Peak2	$w_{1/2}2$
NANOFER STAR*	UPW	0	385	154	253	206		
		29	455	208	294	289		
	RW	0	393	155	289	250		
		29	948	223	251		979	
NANOFER STAR**	UPW	0	334	155	251	207		
		29	417	196	274	255		
	RW	0	386	195	323	281		
		29	806	268	298		884	
Ferrihydrite	UPW	0	302	149	180	151		
		29	343	169	205	170		
	RW	0	411	187	243	210		
		29	808	268	334		663	

The difference of nanoparticle behaviour in UPW and RW was probably caused by natural components in RW, not present in UPW. Although the original powders were formed by nanoparticles, the nanoparticles stabilised themselves by forming aggregates of hydrodynamic diameter larger than 100 nm (100 nm to 1,000 nm) in water environment. The largest aggregates were observed in RW and, therefore, they had stronger tendency to sediment. The sedimentation was even higher because of the difference between the density of RW and UPW.

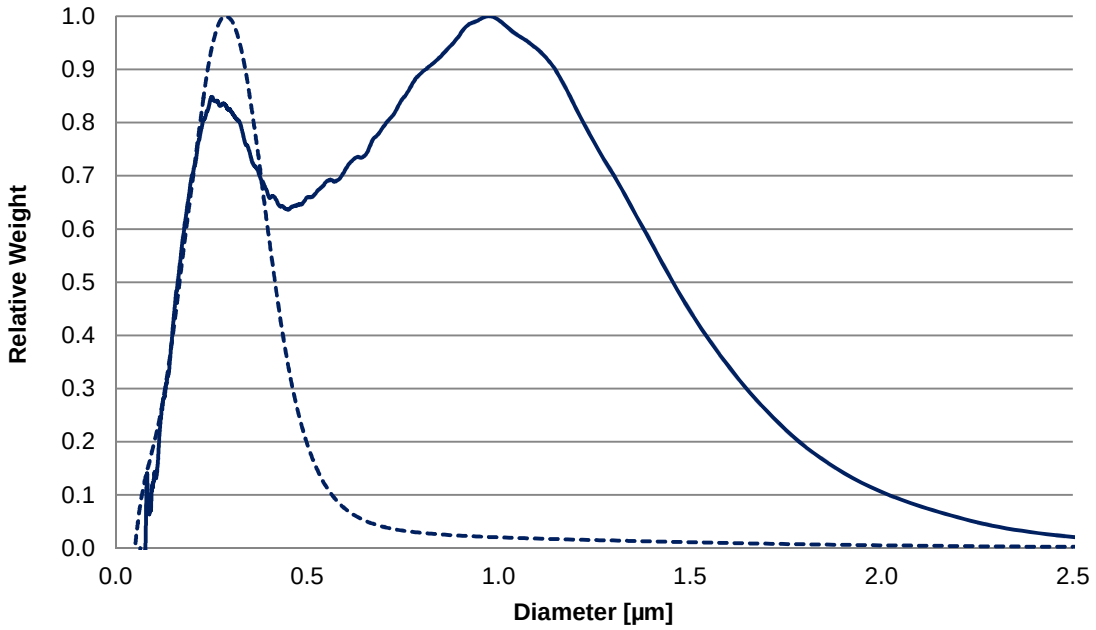

Figure 4.7. Size-distribution by relative weight of NANOFER STAR* in RW: 250 mg/l; at the beginning (dashed line) and after 29 days (solid line); Analysed using DCS.

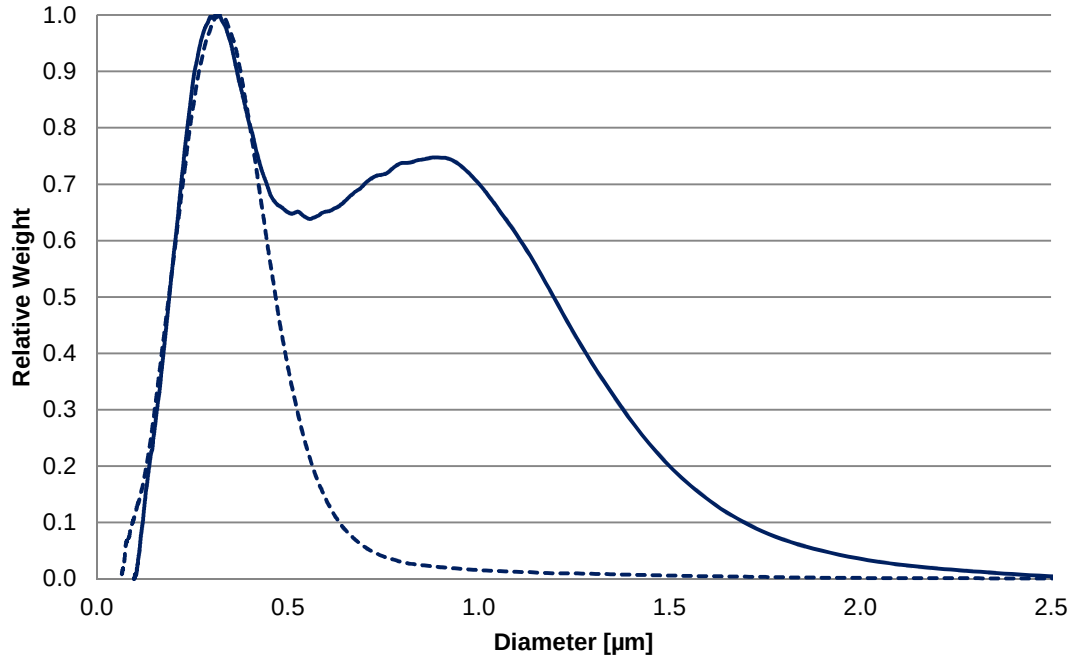

Figure 4.8. Size-distribution by weight of NANOFER STAR in RW: 250 mg/l; at the beginning (dashed line) and after 29 days (solid line); Analysed using DCS.**

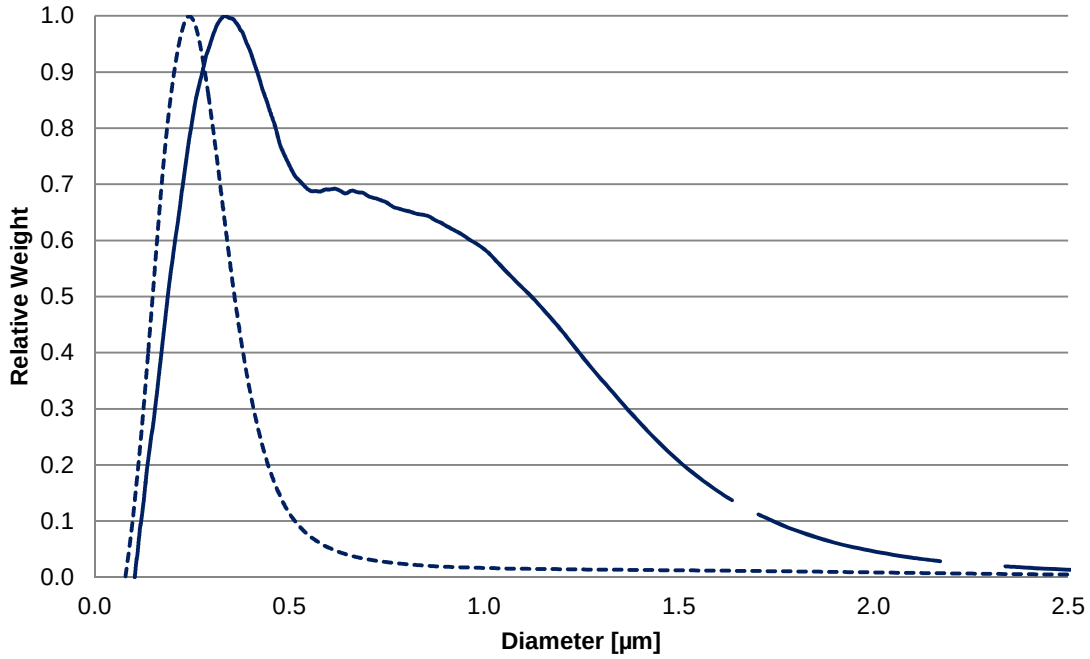

Figure 4.9. DCS size-distribution by weight of ferrihydrite in RW: 250 mg/l; at the beginning (dashed line) and after 29 days (solid line); Analysed using DCS.

Fig. 4.7 and Fig. 4.8 show that there is a difference in ratio between peak of smaller and bigger particles. Most of nanoparticles of older batch (NANOFER STAR*) aggregated into larger particles unlike nanoparticles of fresher batch (NANOFER STAR*). The nanoparticles of fresher batch were more stable. Furthermore, the peak of smaller particles after 29 days and particles at the begging had almost the same position. It refers to two most stable sizes of aggregates. The suspension of ferrihydrite nanoparticles showed both shift of peak and increase in width of size distribution (Fig. 4.9). The increased size of nanoparticles could also refer to their interactions with particulate organic matter or other compounds present in environmental media [37], [38].

The zeta-potential and conductivity of nanoparticle suspensions were measured to determine colloid stability at the begging and after 29 days (Tab 4.4). It was observed that only ferrihydrite nanoparticles were stable in UPW over the time, although the zeta-potential was at the edge of instability range (-30 mV to 30 mV) [30]. The stability of other suspensions was rather poor. Presence of RW compounds destabilized all nanoparticles and their zeta-potential was around -17 mV. The conductivity of suspensions was higher than their original dispersive medium (in UPW and RW),

whereas the difference was higher in RW (about 200 µS/cm) comparing to UPW (about 10 µS/cm).

Table 4.4. Zeta-potential and conductivity of "aging" suspensions: NANOFER STAR (*/) and ferrihydrite in UPW and RW (250 mg/l) at the beginning and after 29 days.**

NP	Medium / Days		Zeta-potential (mV)	Conductivity (µS/cm)
NANOFER STAR*	UPW	0	-18	29
		29	1	3
	RW	0	-17	588
		29	-16	576
NANOFER STAR**	UPW	0	-16	7
		29	-9	21
	RW	0	-17	597
		29	-17	597
Ferrihydrite	UPW	0	-31	7
		29	-30	14
	RW	0	-19	590
		29	-18	586

The "fresh" suspensions were created 14 days after the preparation of "aging" suspensions. The "fresh" suspensions were investigated by DCS and DLS in order to determine their hydrodynamic diameter and to find differences between results from DCS and DLS. The results showed that particle size was smaller (72 nm in average) than the "aging" particles in the day of preparation. The reason might be that the measuring of fresh suspensions was done few hours sooner than measuring of "aging" suspensions and therefore nanoparticle aggregates were smaller.

The colloidal behaviour of metal oxide nanoparticles in presence of NOM studied Saikat Ghosh et al. [39]. They observed that structurally different humic acid (HA) at different concentrations caused both stabilization and destabilization. Nevertheless, the low polar, high molecular weight fractions of HA strongly destabilized the NP suspensions when they were added in small quantity [39]. This corresponds with results in this thesis where the concentration of NOM comparing to NPs was low (2.6 mg/l TOC; 250 mg/l NPs).

The comparison of DCS and DLS showed micron differences in diameter (Tab. 4.5 and Tab. 4.6). Analysis of the diameter of iron-based nanoparticles in media with the same or similar density to water is impossible because of fast nanoparticle sedimentation and low zeta-potential. Therefore, the results seem to be irrelevant. The particle diameter of ferrihydrite in UPW analysed by DLS was in agreement with DCS only because the particles were smaller and their surface was stabilized.

Table 4.5. Hydrodynamic diameter of "fresh" suspensions: NANOFER STAR (*/) and ferrihydrite in UPW and RW (250 mg/l) with and without enrichment by N_2 right after preparation of suspensions; Analysed using DLS method; Z-average (intensity-based mean value for the size; NM (Number Mean of the size, PdI (Polydispersity Index, width parameter).**

NP	Medium / N_2		DLS analysis		
			Z-average (nm)	NM (nm)	PdI
NANOFER STAR*	UPW	No	2395 ± 190	1079 ± 71	0.671 ± 0.074
		Yes	2797 ± 155	1340 ± 117	0.548 ± 0.061
	RW	No	5512 ± 445	622 ± 875	0.480 ± 0.040
		Yes	5400 ± 246	1048 ± 99	0.648 ± 0.025
NANOFER STAR**	UPW	No	3000 ± 570	532 ± 552	0.861 ± 0.099
		Yes	2153 ± 235	151 ± 36	0.631 ± 0.196
	RW	No	7075 ± 1533	307 ± 432	0.708 ± 0.199
		Yes	4608 ± 1018	572 ±800	0.623 ± 0.148
Ferrihydrite	UPW	No	336 ± 5	289 ± 7	0.186 ± 0.013
		Yes	380 ± 6	290 ± 35	0.196 ± 0.007
	RW	No	2293 ± 114	1441 ± 82	0.403 ± 0.022
		Yes	3847 ± 174	1553 ± 204	0.438 ± 0.044

Table 4.6. Hydrodynamic diameters "fresh" suspensions: NANOFER STAR (*/) and ferrihydrite in UPW and RW (250 mg/l) with/without enrichment by N_2 right after preparation of suspensions. Analysed using DCS; WM (Weight Mean by diameter); NM (Number Mean by diameter); Peak (weight Peak diameter); $w_{1/2}$ (width of weight peak diameter at 0.5 its size).**

NP	Medium / N_2		DCS analysis			
			WM (nm)	NM (nm)	Peak (nm)	$w_{1/2}$ (nm)
NANOFER STAR*	UPW	No	276 ± 1	200 ± 1	248 ± 1	181 ± 1
		Yes	269 ± 2	197 ± 3	249 ± 4	180 ± 1
	RW	No	312 ± 1	198 ± 2	266 ± 1	251 ± 2
		Yes	324 ± 3	207 ± 2	274 ± 4	266 ± 9
NANOFER STAR**	UPW	No	272 ± 3	194 ± 4	261 ± 1	239 ± 14
		Yes	279 ± 2	196 ± 1	260 ± 2	184 ± 1
	RW	No	324 ± 11	204 ± 2	257 ± 3	183 ± 2
		Yes	317 ± 6	202 ± 5	280 ± 4	249 ± 16

NP	Medium / N_2		DCS analysis			
			WM (nm)	NM (nm)	Peak (nm)	$w_{1/2}$ (nm)
Ferrihydrite	UPW	No	270 ± 0	198 ± 1	234 ± 0	166 ± 0
		Yes	279 ± 2	201 ± 2	239 ± 1	176 ± 0
	RW	No	328 ± 2	230 ± 1	279 ± 3	221 ± 3
		Yes	317 ± 6	232 ± 2	283 ± 2	249 ± 9

The addition of nitrogen should decrease oxidation rate. Nevertheless, the increase of concentration of dissolved nitrogen complicated the dispersion process in aqueous media. The oxidized particles were more easily dispersed. Finally, no influence of nitrogen on nanoparticle properties was observed thus the results of nitrogen enriched suspension are not reported here. NANOFER STAR samples had very broad size-distribution (PdI) close to 0.7 thus the samples are not suitable for DLS techniques [40]. Conversely, ferrihydrite nanoparticles in UPW had relatively narrow size distribution. Nevertheless, it was not the case of ferrihydrite nanoparticles in RW. Consequently, the larger aggregates with high intensity signal in DLS analysis made detection of smaller particles difficult. This occurred when the Z-average value was much higher than the number mean (NM) value.

4.2.2 Characterization of Suspensions – Experiment at TUL

The physicochemical parameters and particle morphology of "aging" suspensions from the experiment at TUL (Chapter 3.3.2) were investigated. The physicochemical parameters of suspensions and their dispersive media were measured such as pH, ORP, conductivity and temperature. The concentration of dissolved oxygen was measured for dispersive media only because of a risk of oxygen probe damage. The particle morphology of suspensions was measured by AFM and SEM. The chemical parameters of the suspensions were measured two times during the "aging" procedure, 17 days and 28 days after the preparation of the suspensions. The values of pH of suspensions were nearly neutral over the time. The pH was slightly acidic as a normal pH for fresh water lakes [41]. The differences in pH for different suspensions and the dispersive media (UPW, HRW) were not significant. The content of Total Organic Carbon (TOC) in HRW was same as in RW (2.5 mg/l) and the content of total dissolved phosphorus was very low (0.005 mg/l).

The values of ORP showed oxidative conditions (positive values) which had not varied significantly after 17 days and 18 days since preparation of the suspensions. The values of ORP in the dispersive media and the nanoparticle suspensions were nearly the same. It refers that oxidative conditions were caused mainly by dissolved oxygen which was 7.59 ± 0.59 mg/l for UPW and 7.29 ± 0.55 mg/l for HRW. The concentrations of dissolved oxygen were not saturated because the values were below the maximal solubility of oxygen at normal atmospheric pressure and temperatures between 20 °C and 25 °C (9.2 mg/l at 20 °C and 8.4 mg/l at 25 °C) according to Henry's law. The temperature of suspensions and dispersive media was stable and corresponded to laboratory temperature. The values showed that the presence of nanoparticles decreased the conductivity of HRW. The conductivity of UPW was decreased by nanoparticles (besides NANOFER STAR in UPW, 500 mg/l; probably contamination) too, nevertheless the difference between suspension concentrations of 50 mg/l and 500 mg/l was not evident (Tab. 4.7). The conductivity of HRW was half of the conductivity of RW in the experiment at UCD (Tab. 4.8).

Table 4.7. Suspension parameters (pH, ORP) of NANOFERSTAR*, ferrihydrite and Carbo-Iron in UPW or HRW (0 g/ml, 50 g/ml, 500 g/ml) at the beginning and after 17 and 28 days

NP	Medium / Days		pH			ORP		
			0 g/ml	50 g/ml	500 g/ml	0 g/ml	50 g/ml	500 g/ml
NANOFER STAR	UPW	0	6.59 ± 0.43			200 ± 14		
		17		7.14 ± 0.04	6.44 ± 0.22		242 ± 11	196 ± 5
		28		6.93 ± 0.03	6.03 ± 0.10		162 ± 5	180 ± 1
	HRW	0	6.66 ± 0.29			197 ± 7		
		17		6.55 ± 0.15	6.53 ± 0.07		182 ± 7	181 ± 3
		28		6.25 ± 0.19	6.37 ± 0.10		124 ± 2	151 ± 6
Ferrihydrite	UPW	0	6.59 ± 0.43			200 ± 14		
		17		7.08 ± 0.13	6.82 ± 0.06		173 ± 6	170 ± 8
		28		6.44 ± 0.05	7.14 ± 0.03		116 ± 3	134 ± 2
	HRW	0	6.66 ± 0.29			197 ± 7		
		17		6.86 ± 0.04	6.97 ± 0.08		214 ± 3	225 ± 3
		28		6.31 ± 0.23	6.39 ± 0.30		140 ± 5	149 ± 1
Carbo-Iron	UPW	0	6.59 ± 0.43			200 ± 14		
		17		7.25 ± 0.14	6.84 ± 0.11		134 ± 2	264 ± 2
		28		7.35 ± 0.01	6.65 ± 0.01		157 ± 5	161 ± 6
	HRW	0	6.66 ± 0.29			197 ± 7		
		17		6.16 ± 0.22	6.42 ± 0.04		189 ± 7	138 ± 5
		28		6.04 ± 0.30	6.30 ± 0.10		157 ± 3	143 ± 3

Table 4.8. Suspension parameters (conductivity, temperature) for NANOFERSTAR*, ferrihydrite and Carbo-Iron in UPW or HRW (0 mg/l, 50 mg/l, 500 mg/l) at the beginning and after 17 and 28 days

NP	Medium / Days		Conductivity (µS/cm)			Temperature (°C)		
			0 (mg/l)	50 (mg/l)	500 (mg/l)	0 (mg/l)	50 (mg/l)	500 (mg/l)
NANOFER STAR	UPW	0	7.83			22.6		
		17		2	52		22.8	23.4
		28		2	57		23.4	23.2
	HRW	0	187			22.1		
		17		182	165		22.6	23.2
		28		184	167		23.3	23.9
Ferrihydrite	UPW	0	7.83			22.6		
		17		2	2		23.1	23.1
		28		3	3		23.4	23.2
	HRW	0	187			22.1		
		17		182	165		23.0	23.6
		28		184	168		23.4	23.7

NP	Medium / Days		Conductivity (µS/cm)			Temperature (°C)		
			0 (mg/l)	50 (mg/l)	500 (mg/l)	0 (mg/l)	50 (mg/l)	500 (mg/l)
Carbo-Iron	UPW	0	7.83			22.6		
		17		2	2		23.3	23.6
		28		2	2		23.6	23.7
	HRW	0	187			22.1		
		17		181	164		22.9	23.5
		28		184	168		23.3	23.9

The particle size in the suspensions was investigated by DLS, SEM and AFM. The hydrodynamic diameter was impossible to measure by DLS, due to same reason as in the experiment at UCD. The stability of suspensions for DLS measurement was not sufficient. The average particle size of the suspensions was analysed by SEM after 60 days in environmental media and compared to average particle size of pristine nanoparticle powders. The results showed (Tab. 4.9) that average particle size was higher for particles in HRW comparing to UPW. The particles from suspensions were smaller for suspensions of ferrihydrite and Carbo-Iron than pristine particles in powder. Conversely, the pristine nanoparticles of NANOFER STAR* were smaller than in the suspensions.

Table 4.9. The nanoparticle diameter from the SEM and images of NANOFER STAR*, ferrihydrite and Carbon Iron powder after 60 days in environmental media (HRW) or in UPW and diameter of initial nanopowders

NP	Diameter in suspension (nm)	Diameter of initial nanopowder (nm)
NANOFER STAR*	UPW 73 ± 22	46 ± 13
	HRW 89 ± 25	
Ferrihydrite	UPW 70 ± 25	100 ± 30
	HRW 83 ± 23	
Carbo-Iron	UPW 90 ± 46	110 ± 100
	HRW 100 ± 85	

The SEM images (Figs. 4.10 – 4.12) and their size-distribution (Figs. A11 – A22) of suspensions showed that particle size-distribution was relatively narrow except to Carbo-Iron particles.

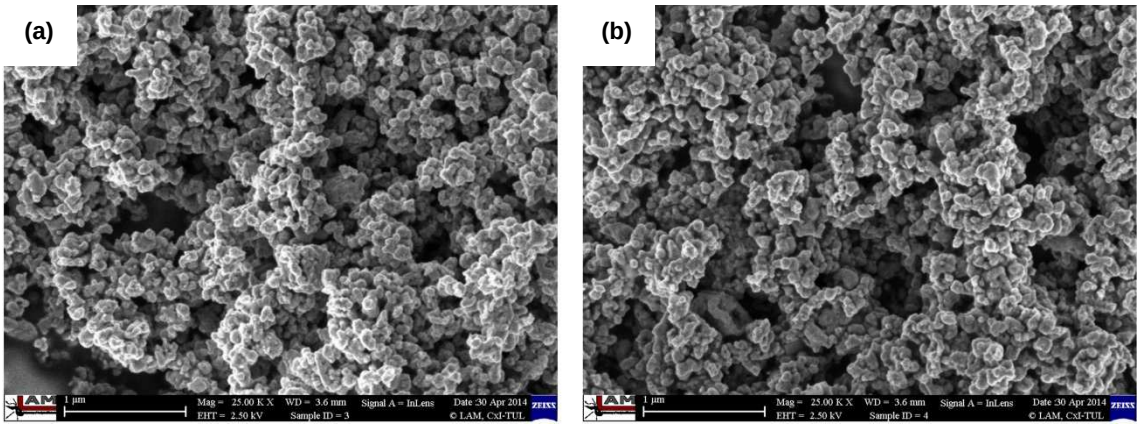

Figure 4.10. SEM images of NANOFER STAR at 25 KX magnification from (a) UPW (b) HRW; 500 mg/l.

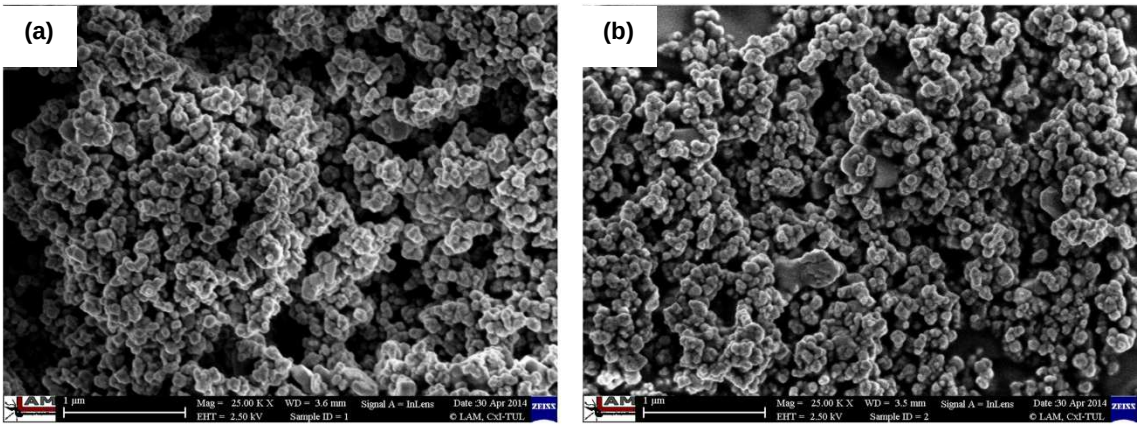

Figure 4.11. SEM images of ferrihydrite at 25 KX magnification from (a) UPW (b) HRW; 500 mg/l.

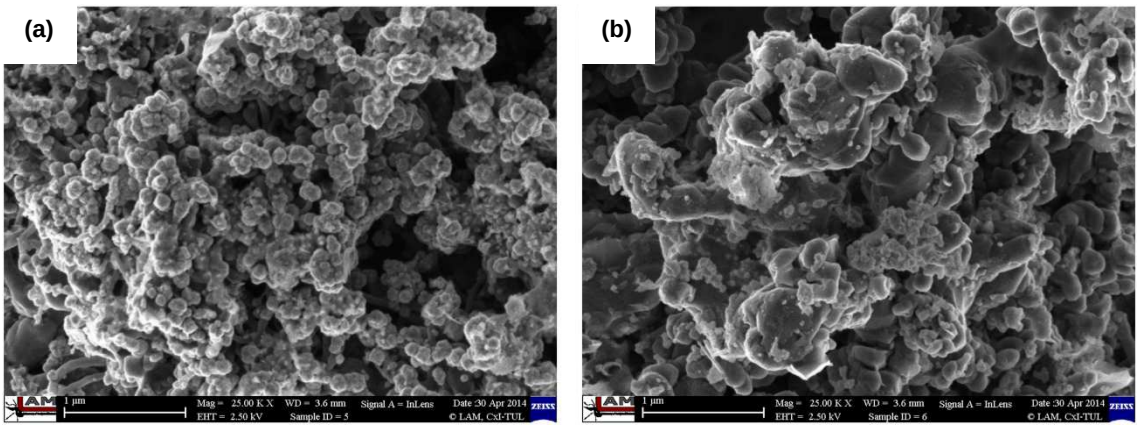

Figure 4.12. SEM images of Carbon-Iron at 25 KX magnification from (a) UPW (b) HRW; 500 mg/l.

The images from AFM did not give any information about particle size-distribution. There were only a few particles recorded (Figs 4.13 – 4.15), and therefore they could not statistically represent whole population. Nevertheless, the images show the size of

single particles or size of aggregates, which was comparable with SEM DSC results in the experiment at UCD.

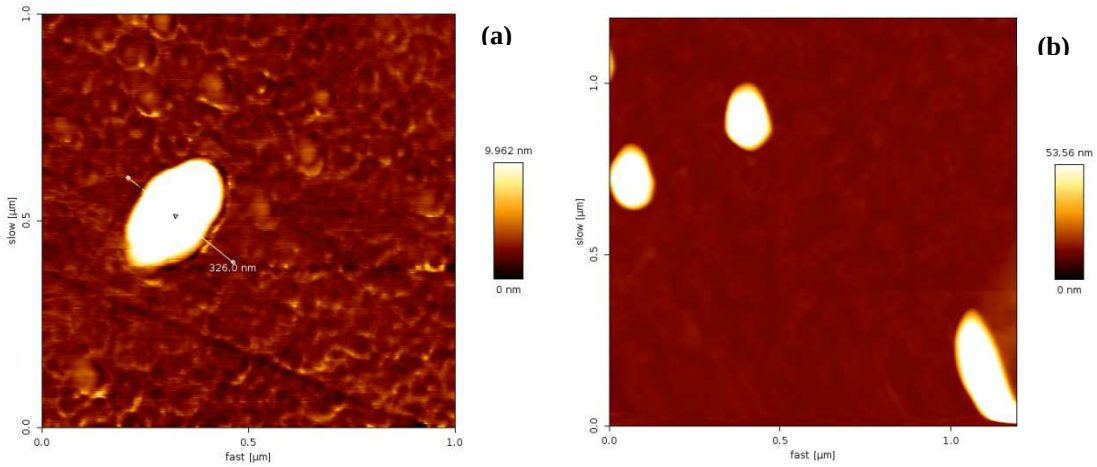

Figure 4.13. AFM images of NANOFER STAR* from UPW (a) and HRW (b)

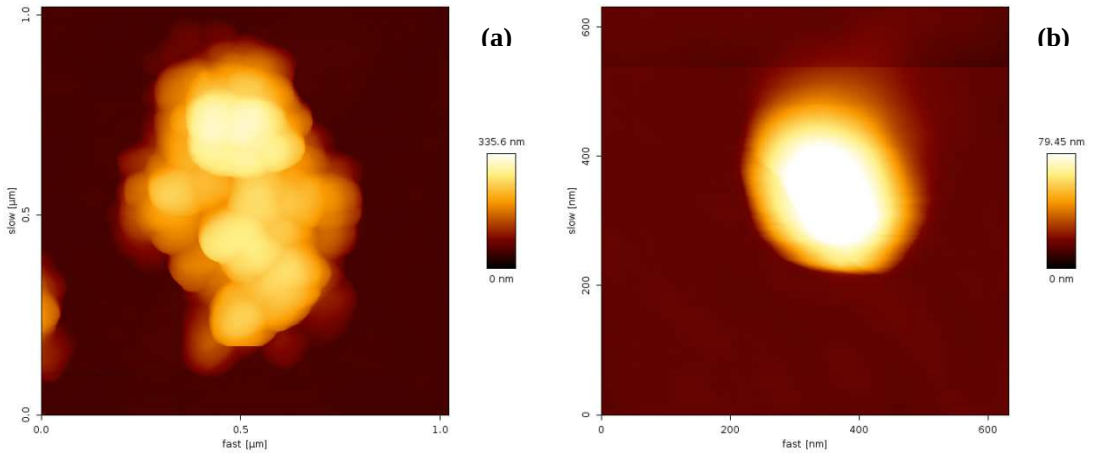

Figure 4.14. AFM images of ferrihydrite from UPW (a) and HRW (b)

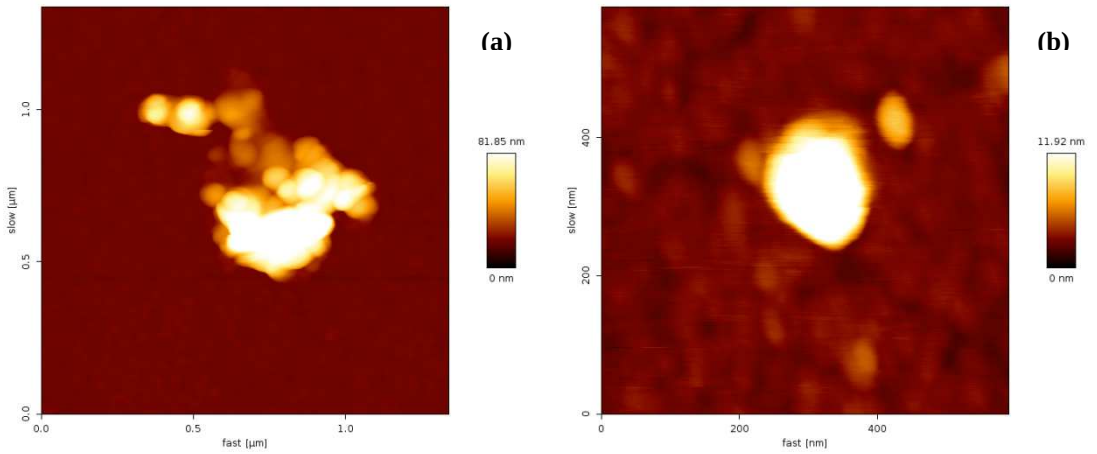

Figure 4.15. AFM images of Carbon-Iron from UPW (a) and HRW (b)

Nowadays, the study of nanomaterial fate in natural environment represents the major challenge because of the experimental difficulties in undertaking studies of particle size at environmentally relevant concentrations typically in the µg/l. It is important to study nanomaterial behaviour in natural aquatic and terrestrial environments because nanomaterial fate can differ significantly from that in synthetic media. [42] Furthermore, the importance to develop a research agenda for aquatic exposure assessment of nanoparticles arises due to number of nanoparticle-containing products entering the market. [38]

4.3 Toxicity Assessment

The toxicity of nanoparticle suspensions in environmental media was studied using model bacteria *E. coli* at the beginning and after 28 day of incubation. The bacterial growth rate (cells/h) was defined by R linear regression of cell density (OD_{600}) versus exposition time. Generally, the results show that *E. coli* growth rate was not affected by nanoparticles dispersed in environmental media at concentrations of 50 mg/l and 500 mg/l comparing to *E. coli* growth rate in UPW containing minimal media at the beginning and after 28 days (Figs. 4.16 and 4.17).

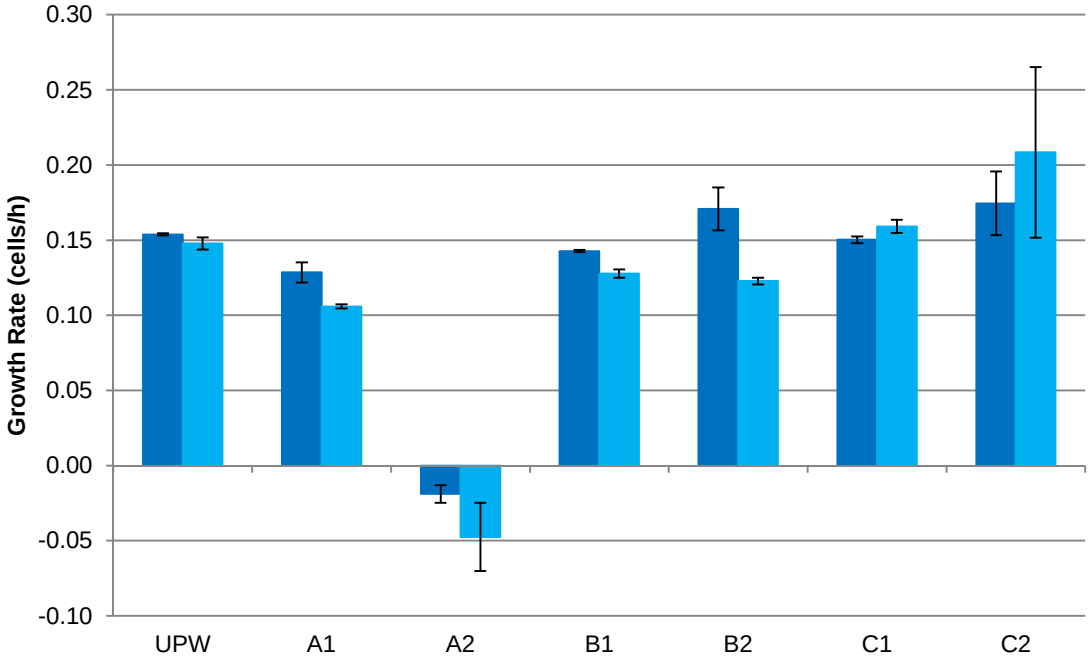

Figure 4.16. *E. coli* growth rate in suspensions of NPs in UPW with minimal media at the beginning (dark blue) and after 28 days (light blue): UPW (control without NPs); 50 mg/l of ferrihydrite (A1); 500 mg/l of ferrihydrite (A2); 50 mg/l of Carbo-Iron (B1); 500 mg/l of Carbo-Iron (B2); 50 mg/l of NANOFER STAR* (C1); 500 mg/l of NANOFER STAR* (C2).

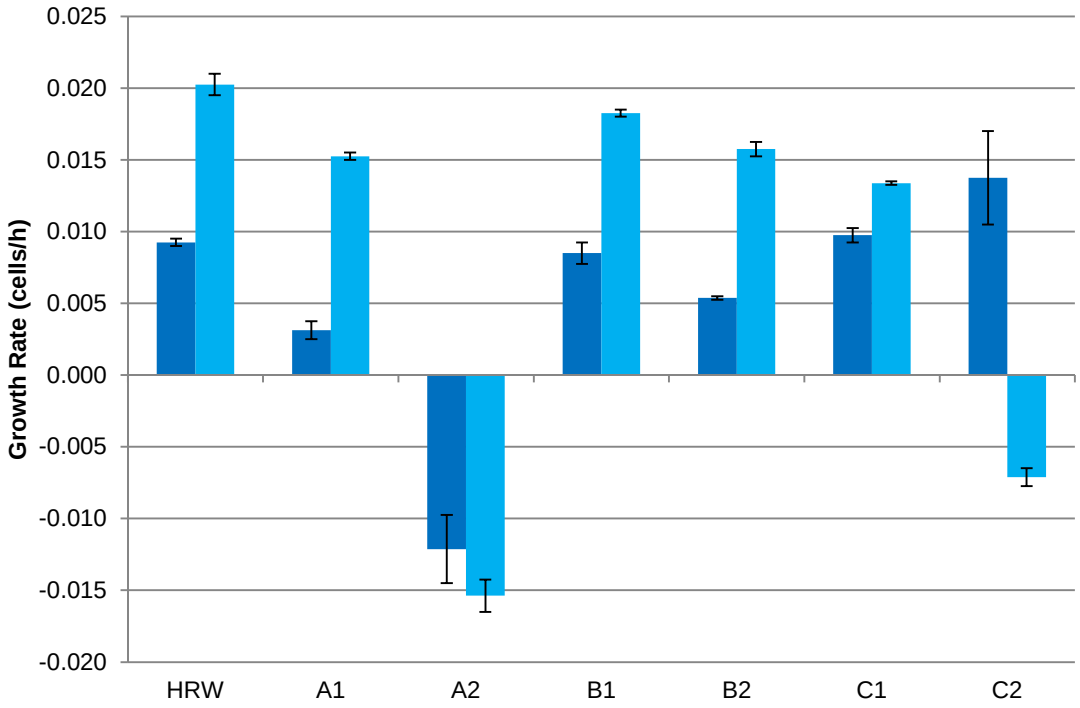

Figure 4.17. *E. coli* growth rate in suspensions of NPs in HRW at the beginning (dark blue) and after 28 days (light blue): HRW (control without NPs); 50 mg/l of ferrihydrite (A1); 500 mg/l of ferrihydrite (A2); 50 mg/l of Carbo-Iron (B1); 500 mg/l of Carbo-Iron (B2); 50 mg/l of NANOFER STAR* (C1); 500 mg/l of NANOFER STAR* (C2).

The reason might be that the amount of bioavailable iron might be very limited in aerobic conditions, because oxygen rapidly oxidizes iron to form sparingly soluble ferric oxides and hydroxides. On the other hand, nZVI particles could quickly attach on the cell surface and interact with membrane ionic or electronic transfers [43]. The effect of 1-hour presence of nanoparticles of Fe_2O_3 and nZVI was much higher toward a mutant *E. coli* lacking antioxidant enzymes than wild type. The authors suggest that the nanoparticles might cause oxidative stress via reactive oxygen species generation and Fenton reaction [44] as demonstrated using a mutant strain of *E. coli* without protective antioxidant enzymes [43]. Significant *E. coli* inactivation was also detected in concentrations of nZVI above 70 mg/l in aerated conditions, [45].

Interestingly, NANOFER STAR* in concentration of 500 mg/l significantly decreased *E. coli* growth rate ($P = 0.0071$) after 28 days in HRW (Fig. 4.17). However, there was no satisfactory explanation for such result, because higher toxicity was expected, if any, for the initial suspension. A dark blackish colour of NANOFER STAR* suspension could interfere with optical density measurement. This was not the case neither when the initial nanoparticle suspension in HRW nor when the nanoparticle suspension in

UPW was used for toxicity assessment. Notably, the dense colour of ferrihydrite suspension (500 mg/l) might interfere with optical density measurement and cause false results (Figs. 4.16 and 4.17). Therefore, the subsamples with *E. coli* exposed to 500 mg/l of ferrihydrite suspensions in UPW and in HRW and 500 mg/l of NANOFER STAR* suspension in HRW were transferred onto agar plates. The size and shape of bacterial colonies were not different to controls without exposition to nanoparticles (Fig. 4.18).

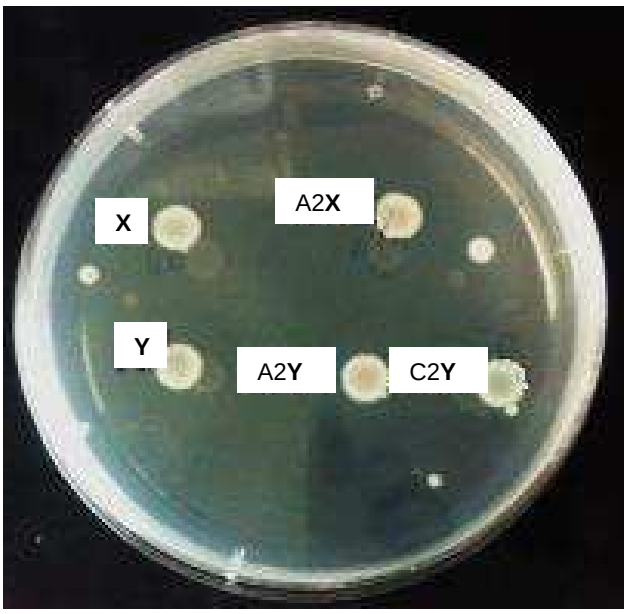

Figure 4.18. *E. coli* growth on agar plate after 6-hour exposition to nanoparticle suspensions: X (UPW only), Y (HRW only), A2X (500 mg/l of ferrihydrite in UPW), A2Y (500 mg/l of ferrihydrite in HRW), C2Y (500 mg/l of NANOFER STAR* in HRW)

To conclude, the tests showed that nanoparticles (Carbon-Iron, NANOFER STAR*) dispersions in UPW were not toxic to *E. coli*. Almost the same results were obtained for nanoparticle suspensions in HRW, except for NANOFER STAR of 500 mg/l concentration. It was not clear what caused significant decrease of *E. coli* growth in ferrihydrite media and in NANOFER STAR in HRW. Nevertheless, the colonies of *E. coli* on Fig. 4.18 shown no difference between controls and bacteria exposed to nanoparticles. More studies are clearly needed to explain the mechanisms of effect of iron-based nanoparticles on bacteria, especially in natural environment.

5 Summary

Iron-based nanoparticles (NANOFER STAR, Carbo-Iron and ferrihydrite) were exposed to environmentally relevant media: river water (RW) and filtered reservoir water (HRW). Furthermore ultra-pure water (UPW) was selected as a blank dispersive medium and the model RW was prepared to mimic the river water. The real RW samples were obtained from St. Annes Park in Dublin (Irish Republic) and the real HRW samples were obtained from Harcov reservoir in Liberec (Czech Republic). Ferrihydrite and NANOFER STAR of different batches (produced in April and June 2013) were dispersed in RW, model RW and UPW in the experiment at UCD at the concentration of 250 mg/l. NANOFER STAR (produced in June 2013, the same batch as in UCD experiment), Carbo-Iron, and ferrihydrite were dispersed in HRW and UPW in two concentrations (50 mg/l and 500 mg/l). Furthermore, the potential toxicity of the iron-based suspensions of nanoparticles in HRW and UPW was investigated on *Escherichia coli* in the experiment at TUL in the beginning and after one-month of suspension aging.

All particles in RW or HRW increased in diameter over the time studied. The dissolved organic matter and other compounds present in environmental media play an important role in behaviour of nanoparticles. The results showed that the environmental components especially affected the stability of nanoparticles. The presence of these components resulted in decrease of electrostatic repulsion and increase in diameter of aggregates based on the electrophoretic light scattering measurements. In consequence of larger size and higher density (about 1 µm and 5 g/ml) of particles, the aggregates and consequent strong sedimentation was observed. An attempt was made to prepare a model water sample mimicking the real river water. The model river water contained similar concentration of humic acids, was of similar ionic strength and pH, still, the analysis showed that model RW was probably too simple to truly mimic the complex composition of real RW system. Therefore, the behaviour of nanoparticle suspensions was rather similar to UPW than to RW.

The suspensions of nanoparticles in environmental media and UPW were analysed by different techniques. The size-distribution of particles in suspensions was investigated by differential centrifugal sedimentation (DCS), dynamic light scattering (DLS) and scanning electron microscopy (SEM). DCS was proved to be appropriate and reliable

method for such task. Conversely, DLS analysis was found to be not successful to reliably measure iron-based particles in aqueous media. The strong sedimentation and unstable nature of particles did not allow collecting consistent data during dynamic scattering. This problem might be solved by stabilization of nanoparticles in suspension in suitable dispersant such as a sucrose.

The particle morphology and size was analysed by SEM and Atom Force Microscopy (AFM). Furthermore, Brunauer-Emmett-Teller (BET) analysis was used to determine specific surface area showing that the pristine nanoparticle powders had surface area between 12 m^2/g and 18 m^2/g. Although AFM is capable to measure particles in aqueous media as well, the dried suspensions were analysed by AFM and SEM. The particles might be affected by drying and could differ from their state in aqueous media. Nevertheless, the images from AFM and SEM confirmed that particles formed more stable aggregates. Moreover, it was observed that the concentration of 500 mg/l was rather high for SEM analysis, because the aggregates did not correspond to the size-distribution detected by DCS and the image analysis was more difficult. The aggregates were too large and pristine aggregates/nanoparticles were not possible to recognize. The elemental composition analysed by Scanning Electron Microscopy/Energy Dispersive X-ray Spectroscopy (SEM/EDS) of nanoparticle powders showed lower content of oxygen in Carbo-Iron powder and higher in ferrihydrite powder. Nevertheless, the single particles of carbon and iron in case of Carbo-Iron were not possible to recognize due to a large interaction region (about 1 µm).

The characterization of dispersive media and the suspensions of nanoparticles were done by pH, Oxidation Reduction Potential (ORP), oxygen concentration, conductivity, temperature, Total Organic Carbon (TOC) and Total Phosphorus (TP) measurements. The parameters showed that RW and HRW had very similar content of TOC, even if HRW was filtered. The content of total dissolved phosphorus was not significant (<0.005 mg/l). The main difference between media was pH and conductivity. RW referred rather to sea water and HRW to freshwater lake. The values of ORP showed that oxidative conditions were dominantly caused by dissolved oxygen; therefore for example strongly reducing agent NANOFER STAR* did not decrease ORP the same way as it is usual in anoxic underground water conditions. The iron-based nanoparticles used in this thesis did not show any toxicity towards *Escherichia coli* when exposed to

nanoparticles in HRW at the beginning of the experiment and after one month of aging process. Iron-based nanoparticles highly sedimented in aqueous environment and this might protect direct contact of their reactive surface with the microorganism. Nevertheless, it does not mean that there is no risk, although iron-based particles commonly occur in natural environment. Further research is needed to gain more knowledge on nanoparticle behaviour in other types of environmental media and their fate.

References

[1] G. J. Horbach, S. Van Den Brule, C. Magkoufopoulou, G. V. D. Papoutsi, L. Leyns, and M. Kirsch-Volders, “The Safety of Nanomaterials: Translation from Academic Research to Industrial and Regulatory Applications,” *J. Transl. Toxicol.*, vol. 1, no. 1, pp. 40–45, Mar. 2014.

[2] A. D. Maynard, “Don’t define nanomaterials,” *Nature*, vol. 475, no. 7354, pp. 31–31, Jul. 2011.

[3] Publications Office, “Commission Recommendation of 18 October 2011 on the definition of nanomaterialText with EEA relevance,” *Off. J. Eur. Union 275*, no. 54, p. 38, Oct. 2011.

[4] E. Gaffet, “Introduction. Nanomaterials and Nanoproducts: World Markets and Human and Environmental Impacts,” in *Nanoethics and Nanotoxicology*, Springer, 2011.

[5] COMM, “COMMUNICATION FROM THE COMMISSION TO THE EUROPEAN PARLIAMENT, THE COUNCIL AND THE EUROPEAN ECONOMIC AND SOCIAL COMMITTEE - Second Regulatory Review on Nanomaterials.” EUROPEAN COMMISION, 10-Mar-2012.

[6] M. Auffan, J. Rose, C. Chanéac, J.-P. Jolivet, A. Masion, M. R. Wiesner, and J.-Y. Bottero, “Surface Reactivity of Manufactured Nanoparticles,” in *Nanoethics and Nanotoxicology*, P. Houdy, M. Lahmani, and F. Marano, Eds. Springer Berlin Heidelberg, 2011, pp. 269–290.

[7] P. Christian, F. Von der Kammer, M. Baalousha, and T. Hofmann, “Nanoparticles: structure, properties, preparation and behaviour in environmental media,” *Ecotoxicol. Lond. Engl.*, vol. 17, no. 5, pp. 326–343, Jul. 2008.

[8] X. Li, H. Xu, Z.-S. Chen, and G. Chen, “Biosynthesis of Nanoparticles by Microorganisms and Their Applications,” *J. Nanomater.*, vol. 2011, p. e270974, Sep. 2011.

[9] A. Hartland, J. R. Lead, V. Slaveykova, D. O’Carroll, and E. Valsami-Jones, “The Environmental Significance of Natural Nanoparticles,” *Nat. Educ. Knowl.*, vol. 4, no. 8, p. 7, 2013.

[10] R. Kessler, “Engineered Nanoparticles in Consumer Products: Understanding a New Ingredient,” *Environ. Health Perspect.*, vol. 119, no. 3, pp. A120–A125, Mar. 2011.

[11] G. A. Waychunas, “Natural nanoparticle structure, properties and reactivity from X-ray studies,” *Powder Diffr.*, vol. 24, no. Special Issue 02, pp. 89–93, 2009.

[12] J. Slunský, “Production of Zero-Valent Iron nanoparticles (nZVI) for in-situ groundwater remediation including recent field scale application and remediation experience,” presented at the Innovative Environmental Assessment and Remediation Technology, Kennesaw State University, USA, 2012.

[13] K. Mackenzie, A. SCHIERZ, A. GEORGI, and F.-D. KOPINKE, “COLLOIDAL ACTIVATED CARBON AND CARBO-IRON – NOVEL MATERIALS FOR IN-SITU GROUNDWATER TREATMENT,” *Glob. NEST J.*, vol. 10, no. 1, pp. 54–61, 2008.

[14] K. Mackenzie, S. Bleyl, A. Georgi, and F.-D. Kopinke, “Carbo-Iron – An Fe/AC composite – As alternative to nano-iron for groundwater treatment,” *Water Res.*, vol. 46, no. 12, pp. 3817–3826, Aug. 2012.

[15] Hiromi Konishi and Huifang Xu, “Nanostructures of Natural Iron Oxide Nanoparticles,” in *Nature’s Nanostructures*, 0 vols., Pan Stanford Publishing, 2012, pp. 75–114.

[16] J. Filip, R. Zboril, O. Schneeweiss, J. Zeman, M. Cernik, P. Kvapil, and M. Otyepka, “Environmental applications of chemically pure natural ferrihydrite,” *Environ. Sci. Technol.*, vol. 41, no. 12, pp. 4367–4374, Jun. 2007.

[17] V. Stone, B. Nowack, A. Baun, N. van den Brink, F. von der Kammer, M. Dusinska, R. Handy, S. Hankin, M. Hassellöv, E. Joner, and T. F. Fernandes, “Nanomaterials for environmental studies: Classification, reference material issues, and strategies for physico-chemical characterisation,” *Sci. Total Environ.*, vol. 408, no. 7, pp. 1745–1754, Mar. 2010.

[18] I. A. Mudunkotuwa and V. H. Grassian, “The devil is in the details (or the surface): impact of surface structure and surface energetics on understanding the behavior of nanomaterials in the environment,” *J. Environ. Monit. JEM*, vol. 13, no. 5, pp. 1135–1144, May 2011.

[19] M. A. Maurer-Jones, I. L. Gunsolus, C. J. Murphy, and C. L. Haynes, “Toxicity of engineered nanoparticles in the environment,” *Anal. Chem.*, vol. 85, no. 6, pp. 3036–3049, 2013.

[20] “Nanometrology for Practical Applications.” Australian Government, National Measurement Institute, 2013.

[21] R. García, *Amplitude Modulation Atomic Force Microscopy*. John Wiley & Sons, 2011.

[22] “Atomic force microscopy (AFM),” *Laboratoire interdisciplinare de Physique*. [Online]. Available: http://www-liphy.ujf-grenoble.fr/Microscopie-a-force-atomique-AFM?lang=en.

[23] Y. G. Kuznetsov and A. McPherson, “Atomic Force Microscopy in Imaging of Viruses and Virus-Infected Cells.” [Online]. Available: http://mmbr.asm.org. [Accessed: 11-May-2014].

[24] R. Egerton, *Physical Principles of Electron Microscopy: An Introduction to TEM, SEM, and AEM*. Springer, 2006.

[25] “Machine Variables,” *Scanning Electron Microscope (SEM)*. [Online]. Available: http://131.229.88.77/microscopy/semvar.html.

[26] CPS Instruments, “CPS Disk Centrifuge, Nano Particle Size Analysis.” 2007.

[27] Sigma-Aldrich Corp., “Rate-Zonal Centrifugation,” *Centrifugation Separations*. [Online]. Available: http://www.sigmaaldrich.com/technical-documents/articles/biofiles/centrifugation-separations.html.

[28] “Disc Centrifuge,” *CPS Instruments Europe*. [Online]. Available: http://www.cpsinstruments.eu/centrifuge.html.

[29] M. Jones, “Dynamic light scattering,” *Wikipedia*, 2010. [Online]. Available: http://en.wikipedia.org/wiki/Dynamic_light_scattering.

[30] Malvern, “Zeta potential - An introduction in 30 minutes.” 2014.

[31] “Biomembranes - Methodologies,” *Institute of Molecular Medicine*. [Online]. Available: http://www.biochemistry-imm.org/cat.php?catid=115.

[32] P. Pitter, *Hydrochemie*, 4th ed. Praha: VŠCHT Praha, 2009.

[33] “multi N/C® 3100,” *AnalytikJena*. [Online]. Available: http://analytikjenauk.co.uk/multi3100.html.

[34] P. Houdy, M. Lahmani, and F. Marano, *Nanoethics and Nanotoxicology*. Springer, 2011.

[35] NANO IRON, s.r.o, “NANOFER STAR: air-stable nZVI powder.” [Online]. Available: http://www.nanoiron.cz/en/nanofer-star.

[36] “Conductivity, Salinity and Total Dissolved Solids,” *Environmental Measurement Systems*. [Online]. Available: http://www.fondriest.com/environmental-measurements/parameters/water-quality/conductivity-salinity-tds/. [Accessed: 14-May-2014].

[37] G. R. Aiken, H. Hsu-Kim, and J. N. Ryan, “Influence of dissolved organic matter on the environmental fate of metals, nanoparticles, and colloids,” *Environ. Sci. Technol.*, vol. 45, no. 8, pp. 3196–3201, Apr. 2011.

[38] A. Praetorius, R. Arvidsson, S. Molander, and M. Scheringer, “Facing complexity through informed simplifications: a research agenda for aquatic exposure assessment of nanoparticles,” *Environ. Sci. Process. Impacts*, vol. 15, no. 1, pp. 161–168, Jan. 2013.

[39] S. Ghosh, H. Mashayekhi, B. Pan, P. Bhowmik, and B. Xing, “Colloidal Behavior of Aluminum Oxide Nanoparticles As Affected by pH and Natural Organic Matter,” *Langmuir*, vol. 24, no. 21, pp. 12385–12391, Nov. 2008.

[40] Malvern Instruments, “Dynamic light scattering common terms defined.” 2011.

[41] “pH of Water,” *Environmental Measurement Systems*. [Online]. Available: http://www.fondriest.com/environmental-measurements/parameters/water-quality/ph/. [Accessed: 14-May-2014].

[42] G. E. Batley, J. K. Kirby, and M. J. McLaughlin, “Fate and risks of nanomaterials in aquatic and terrestrial environments,” *Acc. Chem. Res.*, vol. 46, no. 3, pp. 854–862, 2013.

[43] M. Auffan, W. Achouak, J. Rose, M.-A. Roncato, C. Chanéac, D. T. Waite, A. Masion, J. C. Woicik, M. R. Wiesner, and J.-Y. Bottero, “Relation between the redox state of iron-based nanoparticles and their cytotoxicity toward Escherichia coli,” *Environ. Sci. Technol.*, vol. 42, no. 17, pp. 6730–6735, Sep. 2008.

[44] A. Ševců, El-Temsah, E. J. Joner, M. Černík, “Oxidative Stress Induced in Microorganisms by Zero-valent Iron Nanoparticles,” *Microbes Environ.*, vol. 26, no. 4, pp. 271–281, 2011.

[45] C. Lee, J. Y. Kim, W. I. Lee, K. L. Nelson, J. Yoon, and D. L. Sedlak, “Bactericidal Effect of Zero-Valent Iron Nanoparticles on Escherichia coli,” *Environ. Sci. Technol.*, vol. 42, no. 13, pp. 4927–4933, Jul. 2008.

Appendix

Experiment at UCD

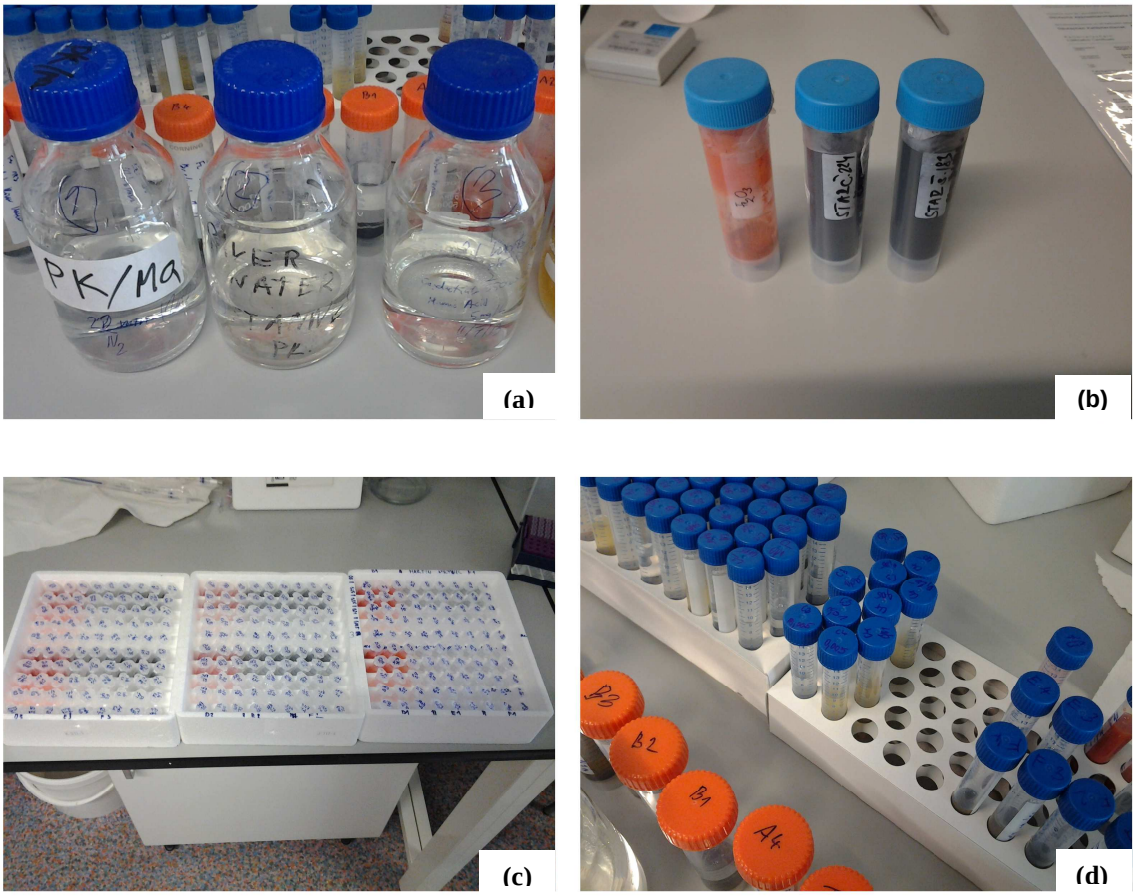

Figure A1. Images of the samples for the experiment at UCD: dispersive environment, from left UPW, RW, model RW (a); nanopowders, from left ferrihydrite, NANOFER STAR*, NANOFER STAR (b); suspensions in vials, N_2 enrichment (c); suspensions Falcon tubes (d)**

Experiment at TUL

(a)

(b)

(c)

Figure A2. Images of the Harcov reservoir: the Harcov dam and Jested hill (a); location of WHR samples (b); samples of WHR in PET bottles (c).

(a)

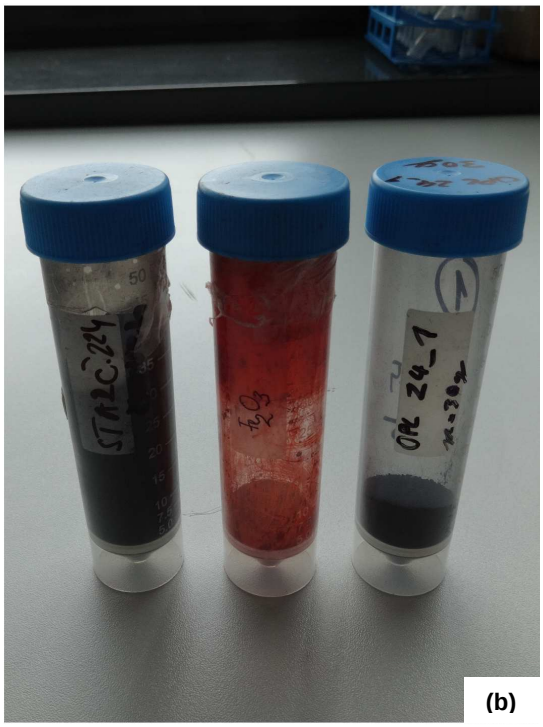

(b)

(c)

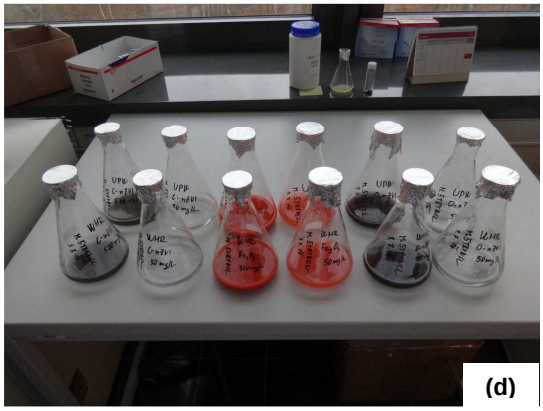

(d)

Figure A3. Suspension preparation from UPW, HRW and NANOFER STAR*, ferrihydrite and Carbo-Iron: Filtration of HRW (a); From left NANFER STAR, ferrihydrite, Carbo-Iron nanopowders (b); Homogenization of stock suspensions (c); "Aging" suspensions (d).

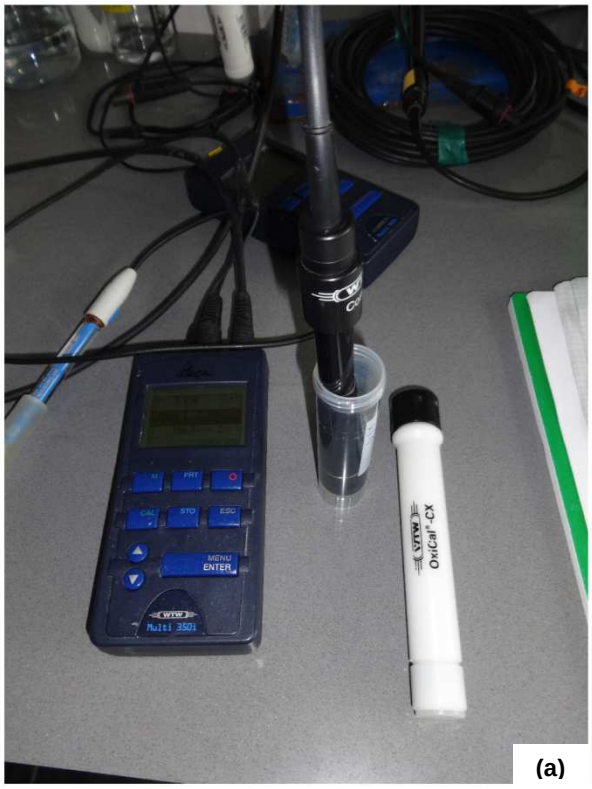

(a)

(b)

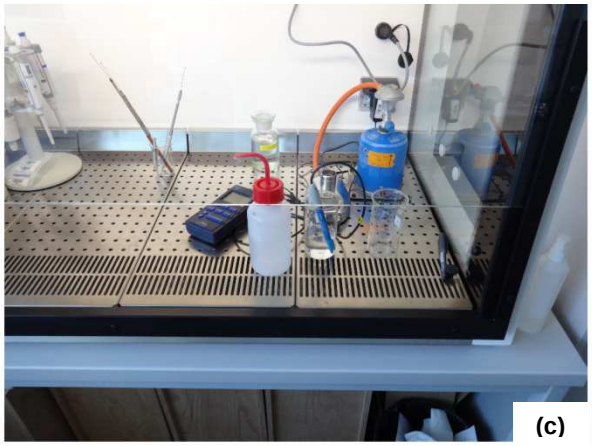

(c)

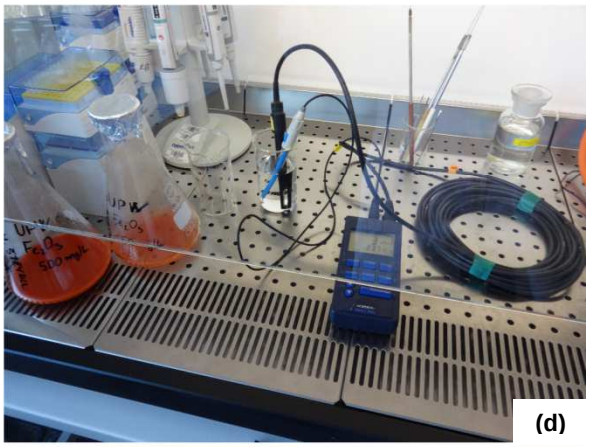

(d)

Figure A4. Characterization of suspensions or dispersive media: dissolved oxygen (a); size-distribution by DLS (b); pH (c); conductivity and ORP (d).

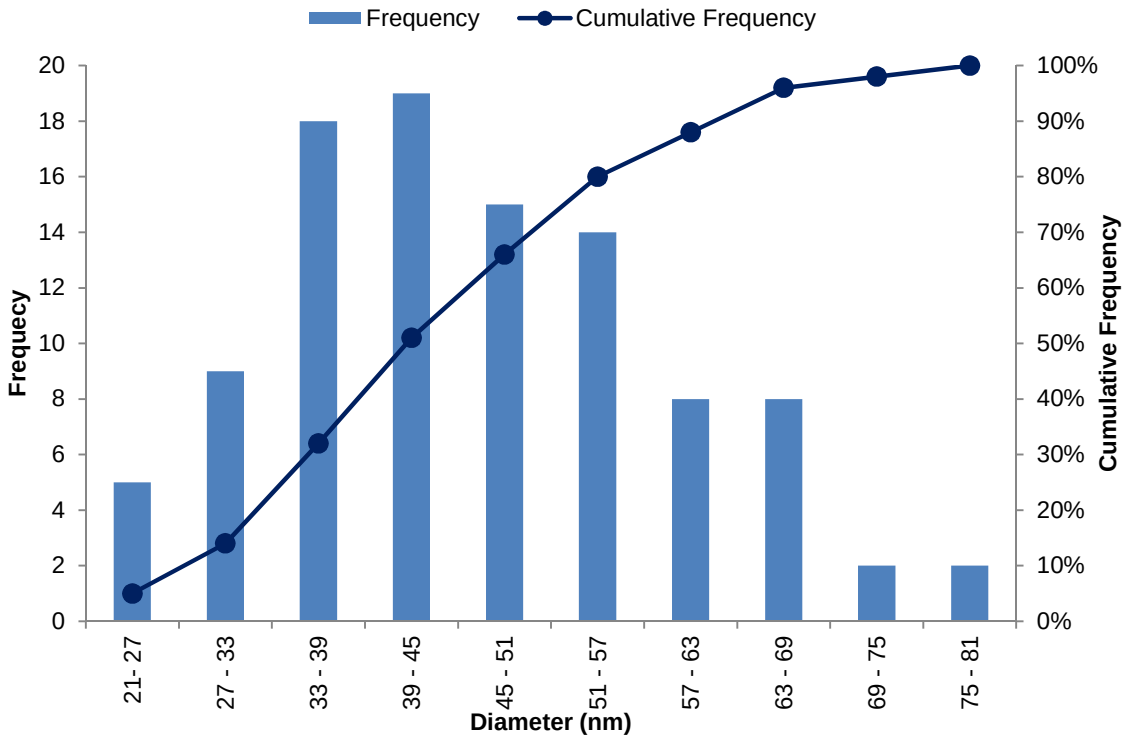

Figure A5. Histogram of size frequency of NANOFER STAR*

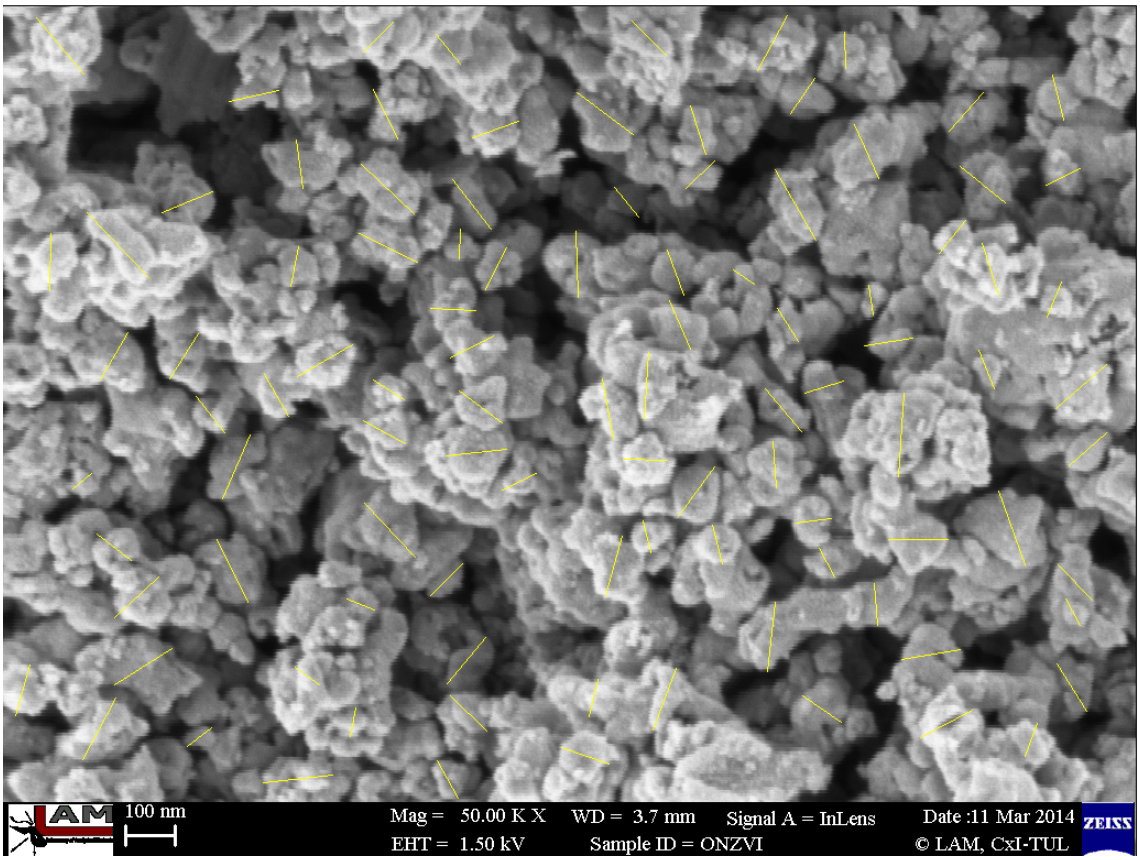

Figure A6. SEM image of NANOFER STAR* used for diameter measuring in the ImageJ software

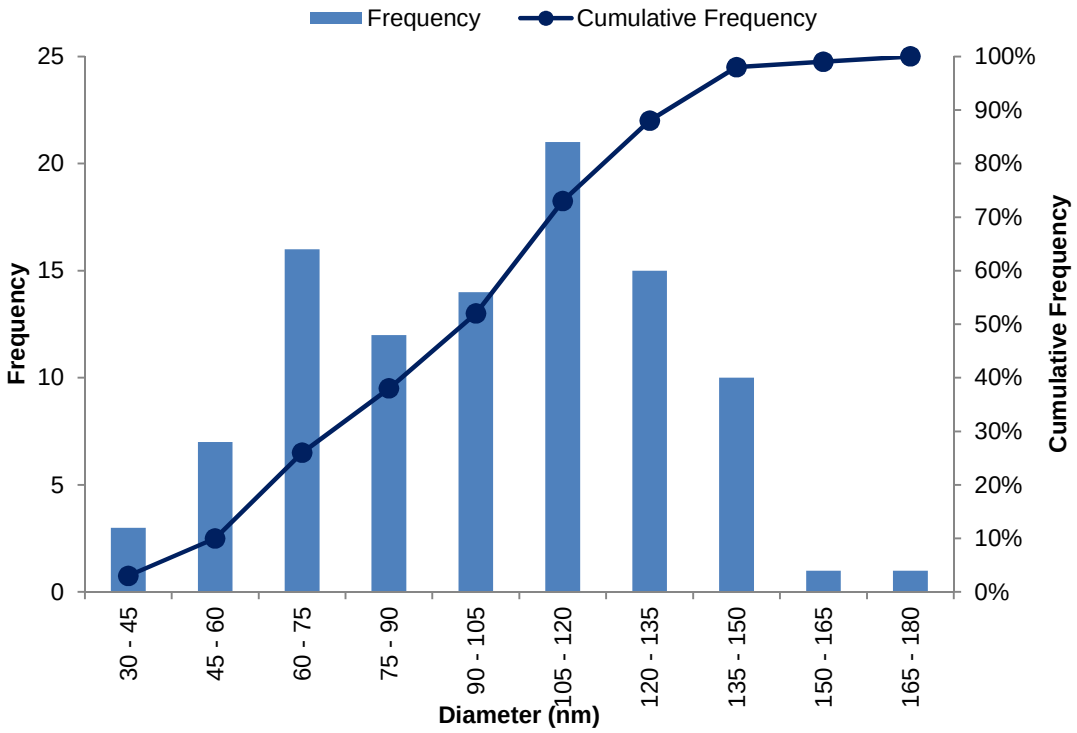

Figure A7. Histogram of size frequency of ferrihydrite

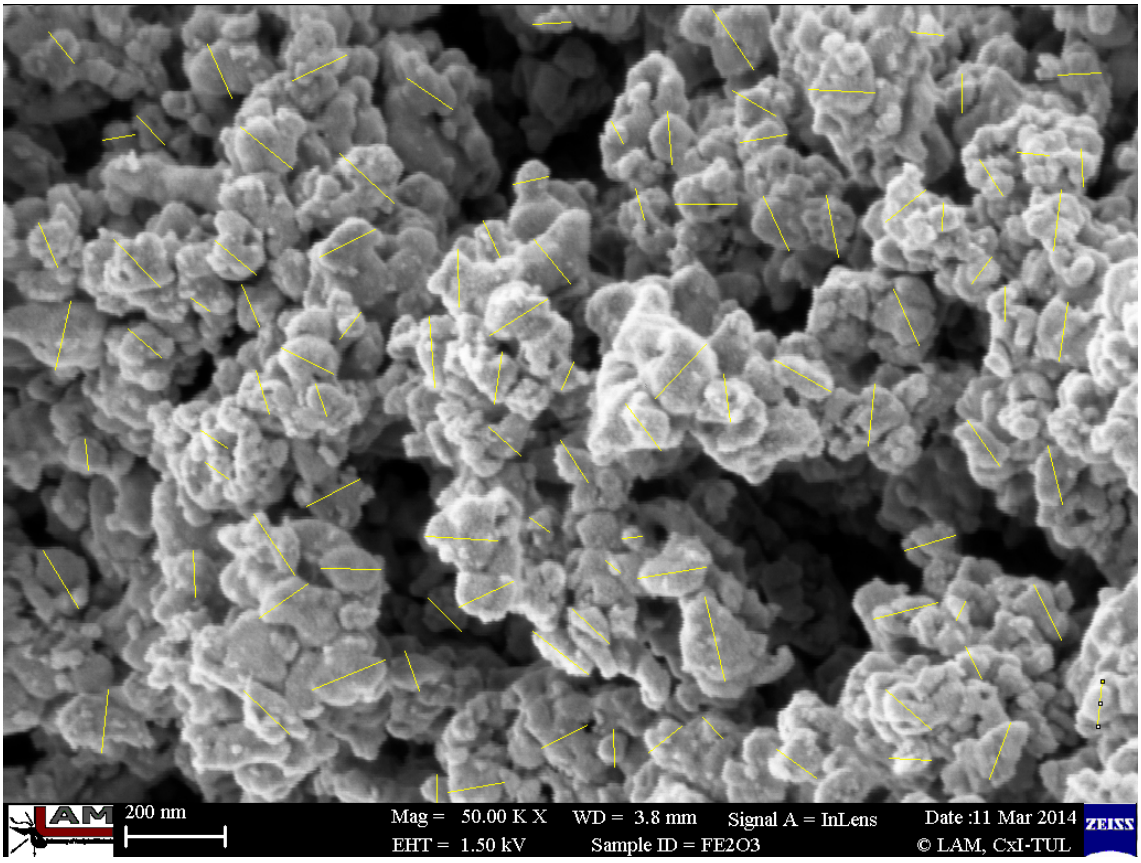

Figure A8. SEM image of ferrihydrite used for diameter measuring in the ImageJ software

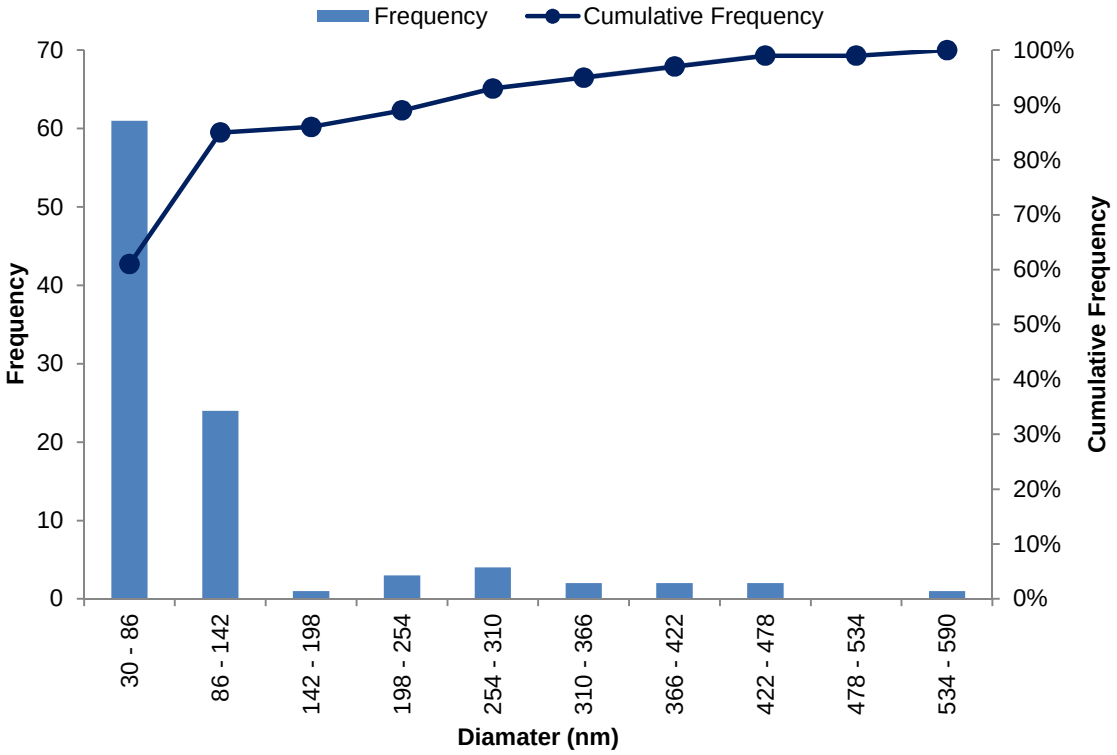

Figure A9. Histogram of size frequency of Carbo-Iron

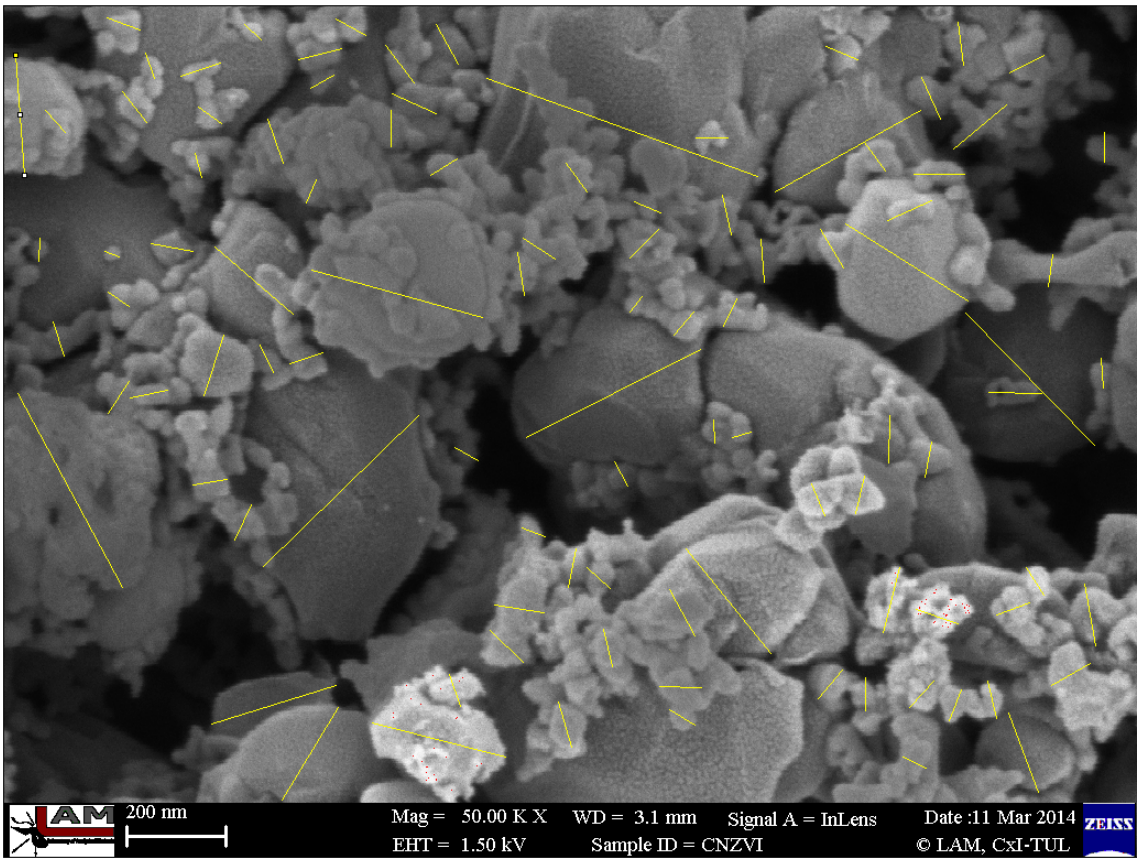

Figure A10. SEM image of Carbon-Iron used for diameter measuring in the ImageJ software

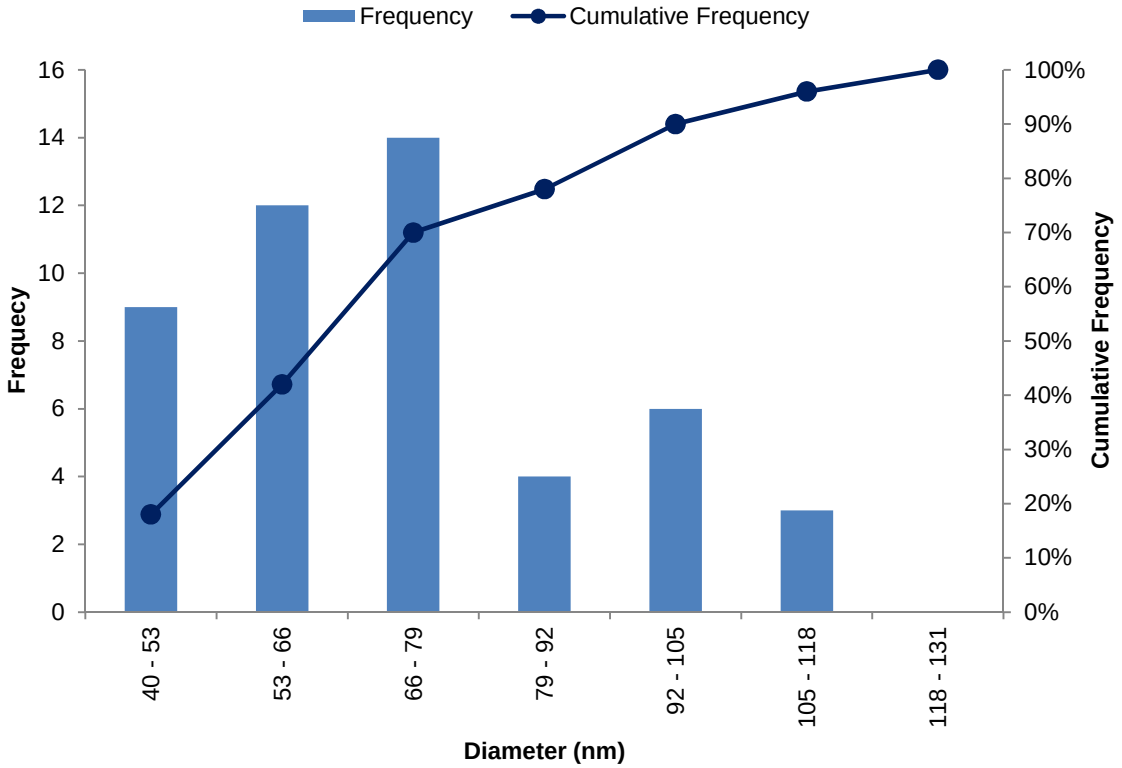

Figure A11. Histogram of size and frequency of NANOFER STAR* from UPW

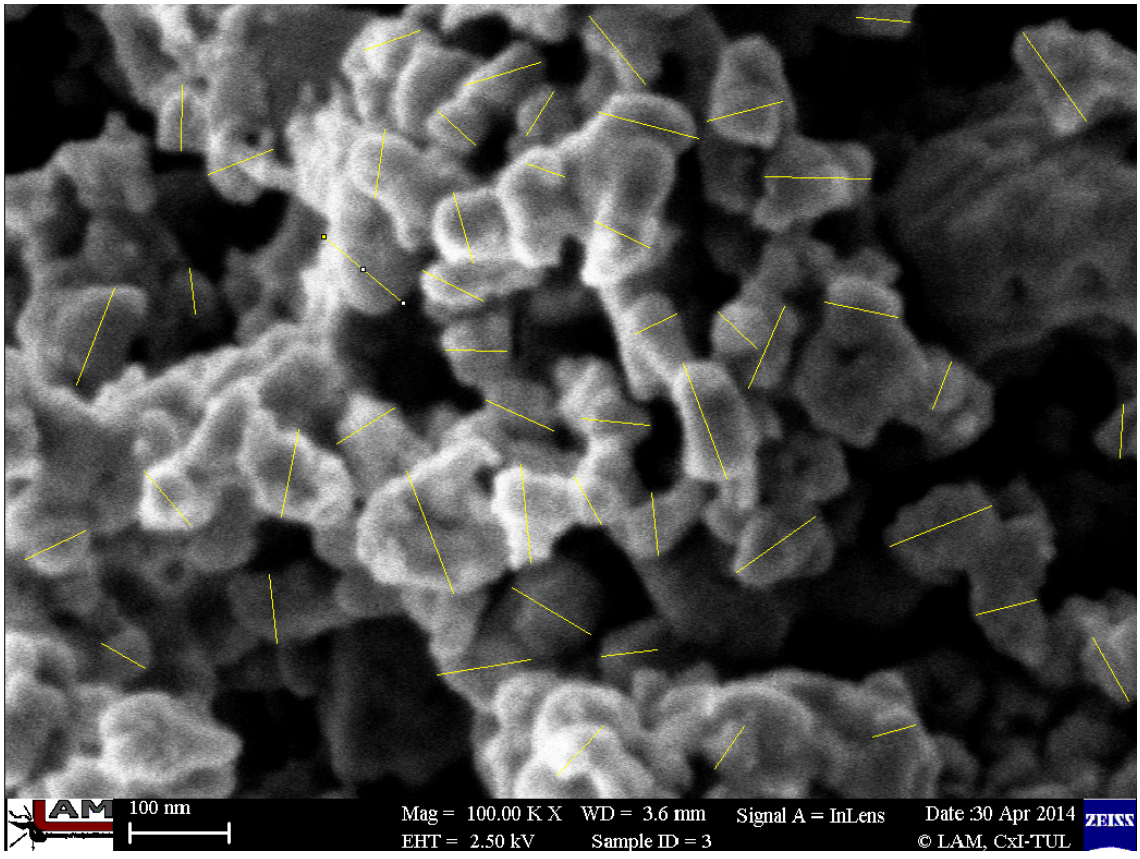

Figure A12. SEM image of NANOFER STAR* from UPW used for diameter measuring in the ImageJ software

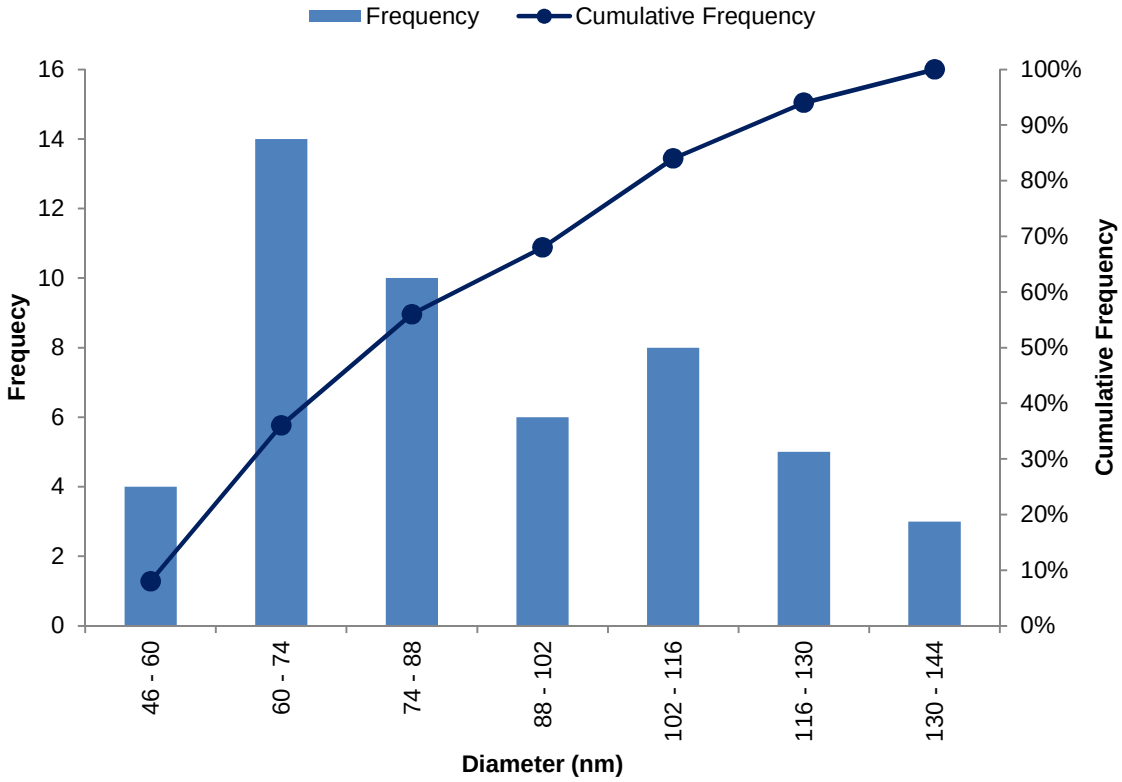

Figure A13. Histogram of size and frequency of NANOFER STAR* from HRW

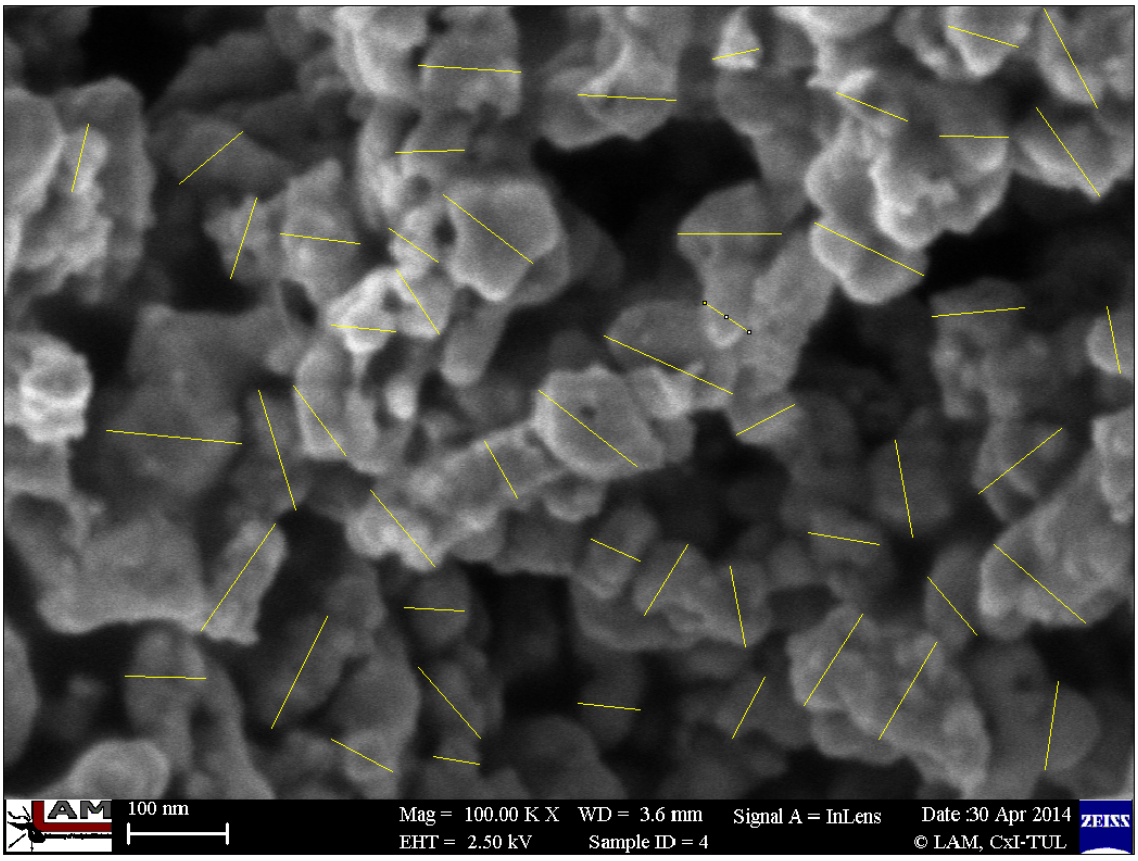

Figure A14. SEM image of NANOFER STAR* from HRW used for diameter measuring in the ImageJ software

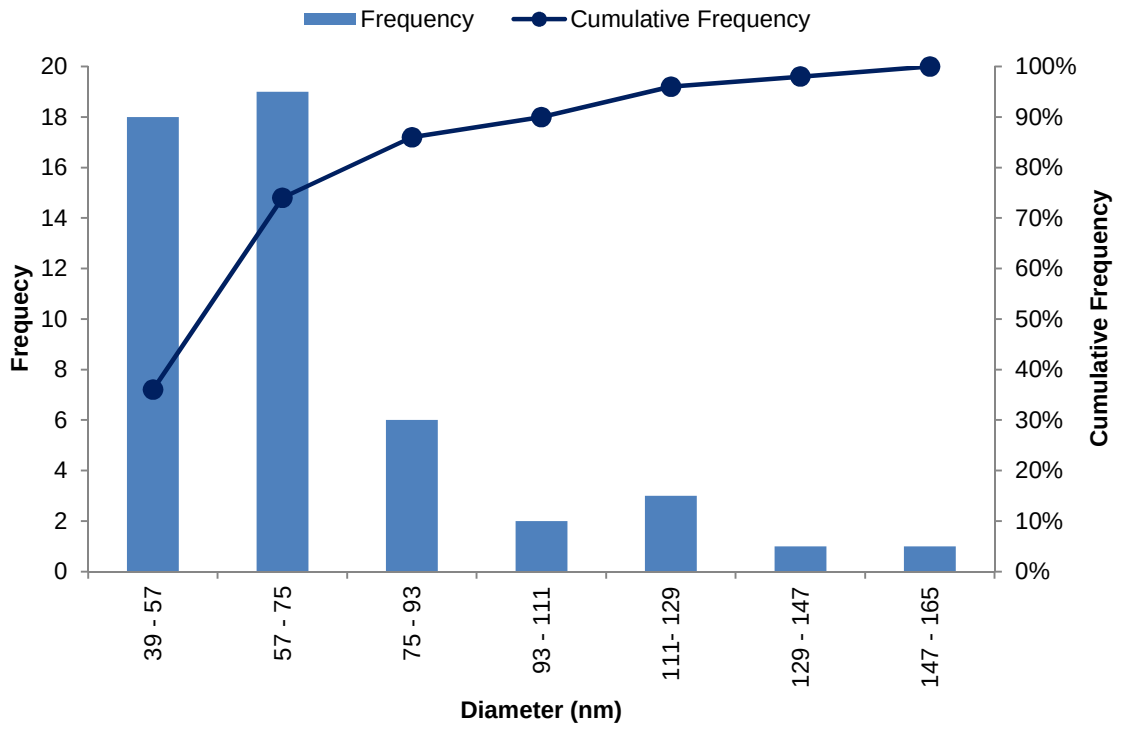

Figure A15. Histogram of size frequency of ferrihydrite from UPW

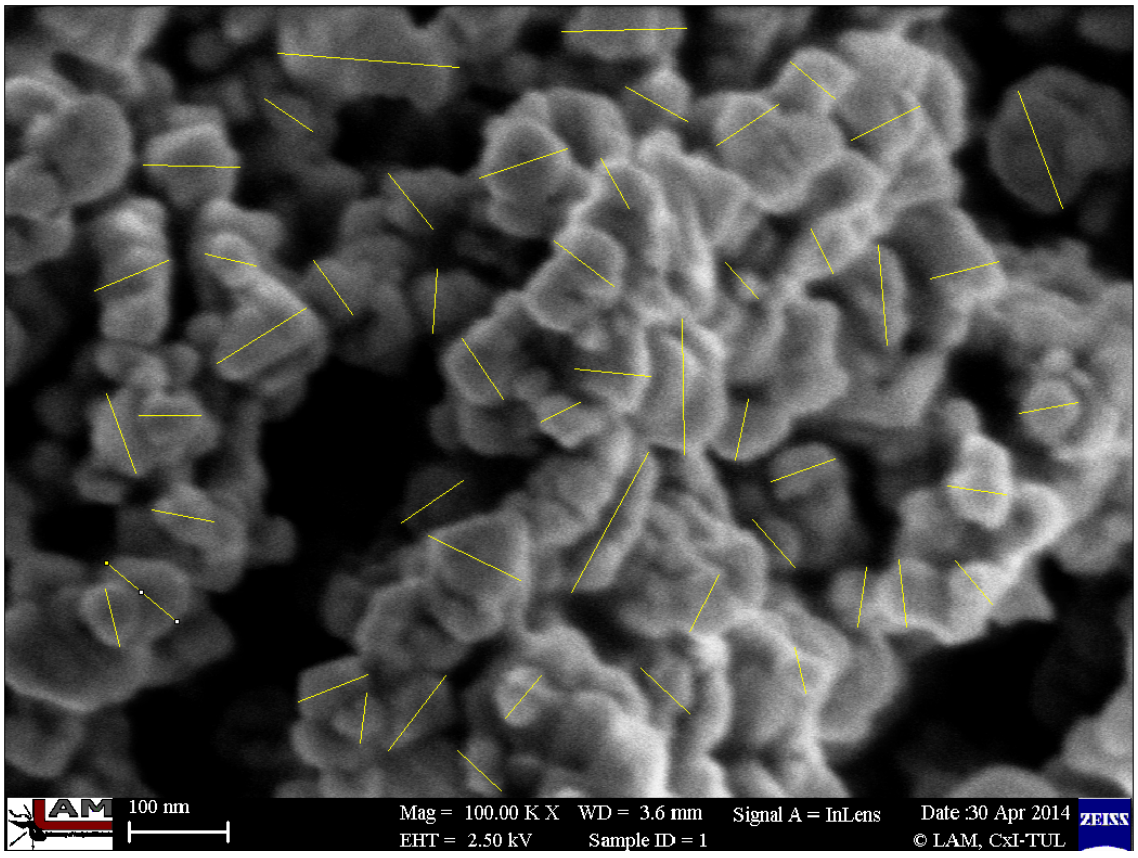

Figure A16. SEM image of ferrihydrite from UPW used for diameter measuring in the ImageJ software

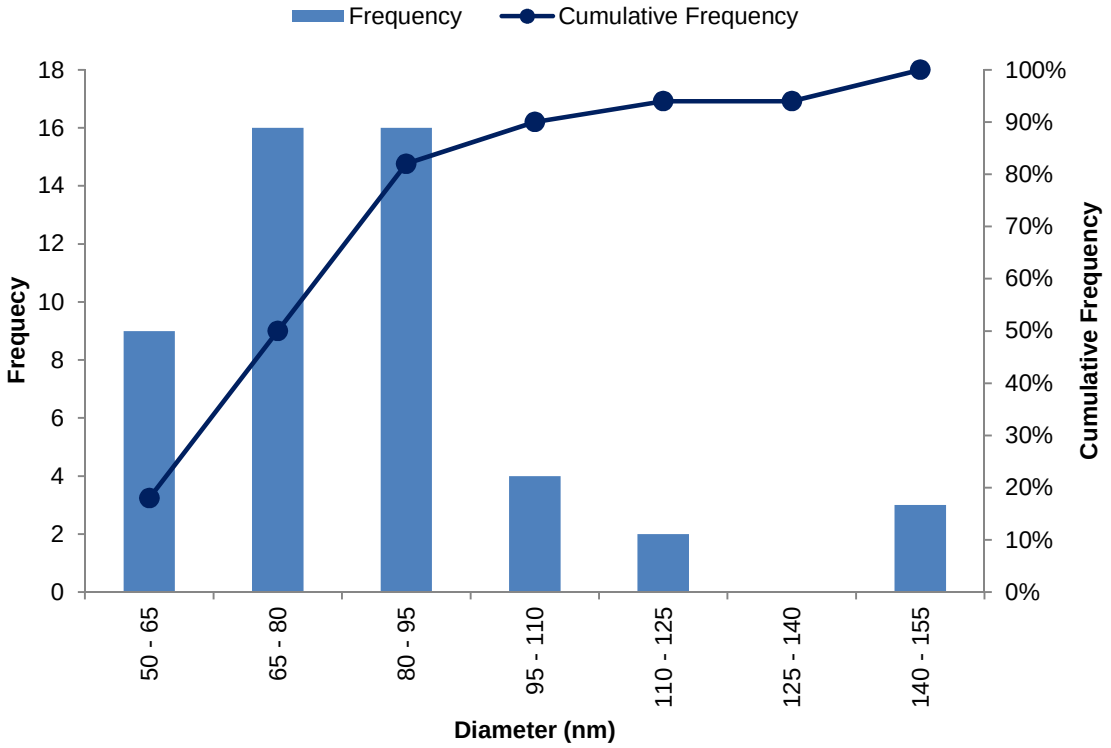

Figure A17. Histogram of size frequency of ferrihydrite from HRW

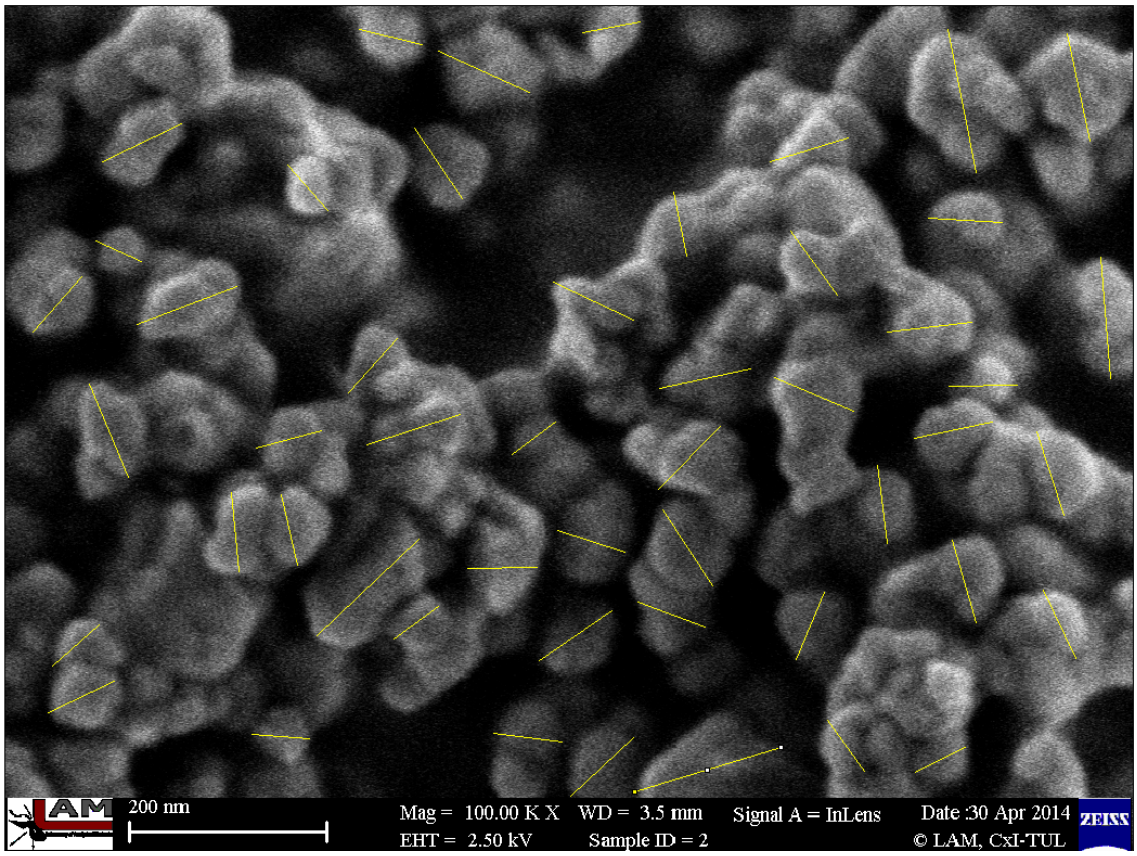

Figure A18. SEM image of ferrihydrite from HRW used for diameter measuring in the ImageJ software

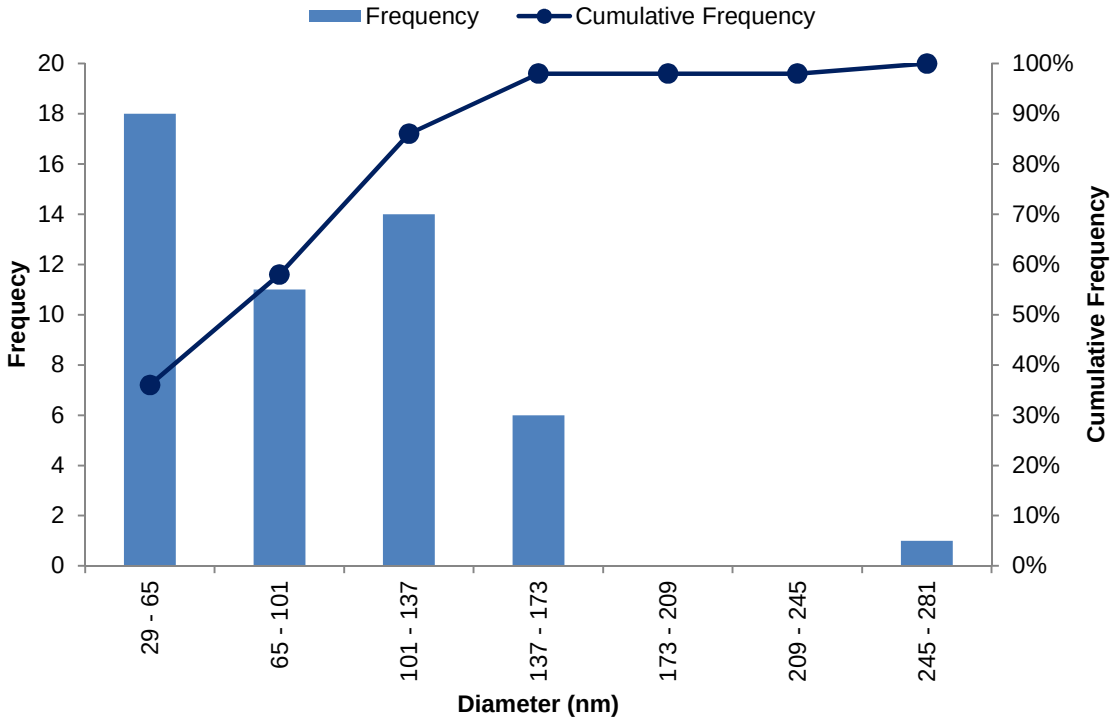

Figure A19. Histogram of size frequency of Carbo-Iron from UPW

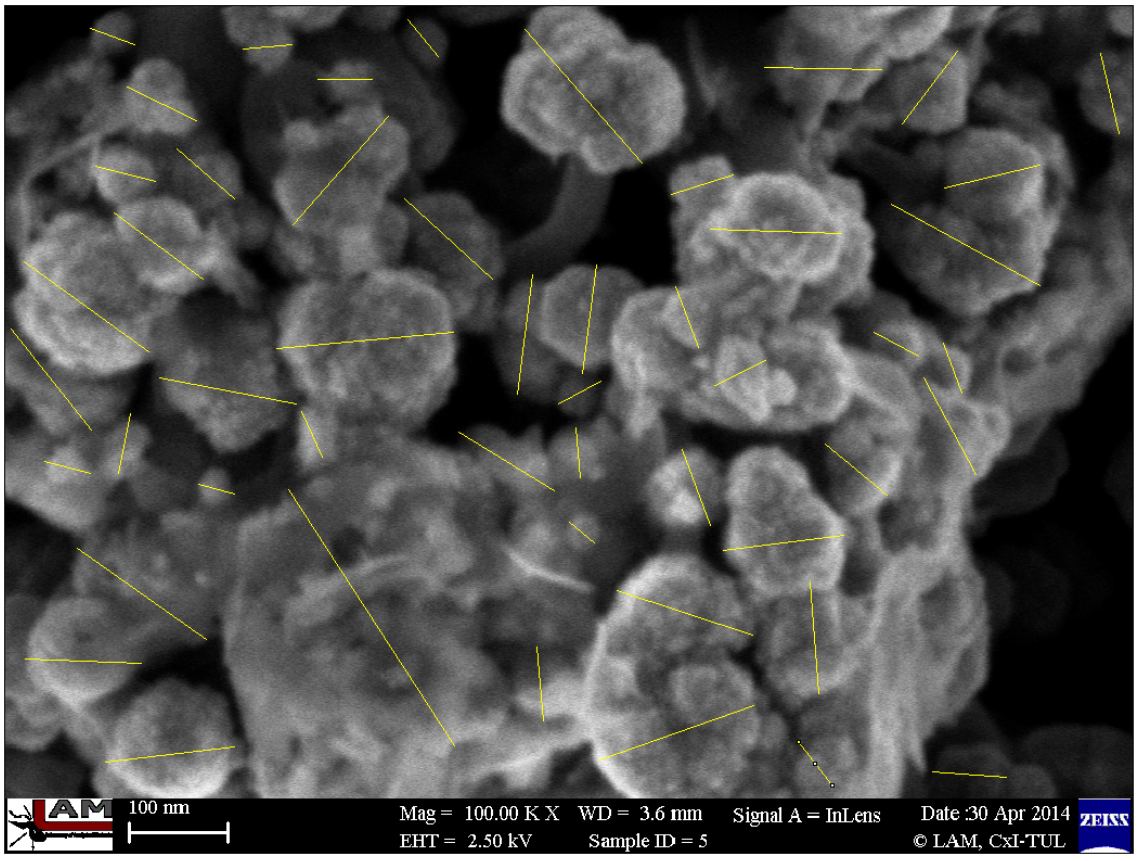

Figure A20. SEM image of Carbon-Iron from UPW used for diameter measuring in the ImageJ software

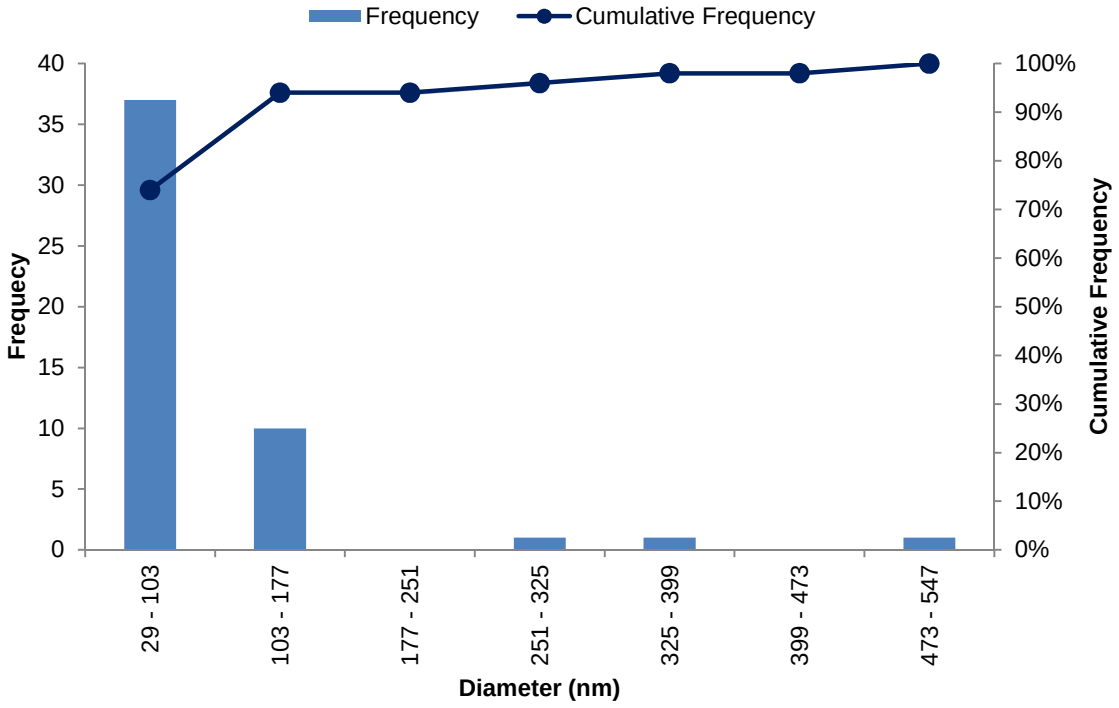

Figure A21. Histogram of size frequency of Carbo-Iron from HRW

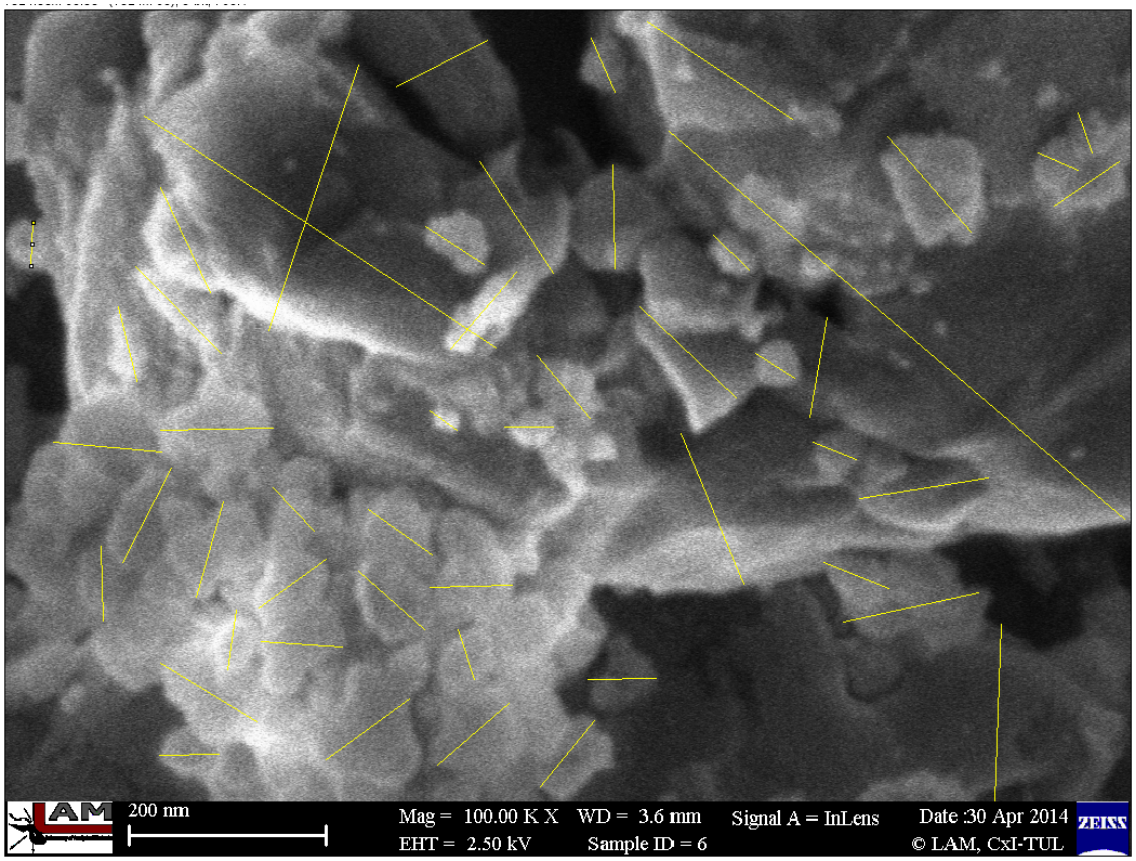

Figure A22. SEM image of Carbon-Iron from HRW used for diameter measuring in the ImageJ software

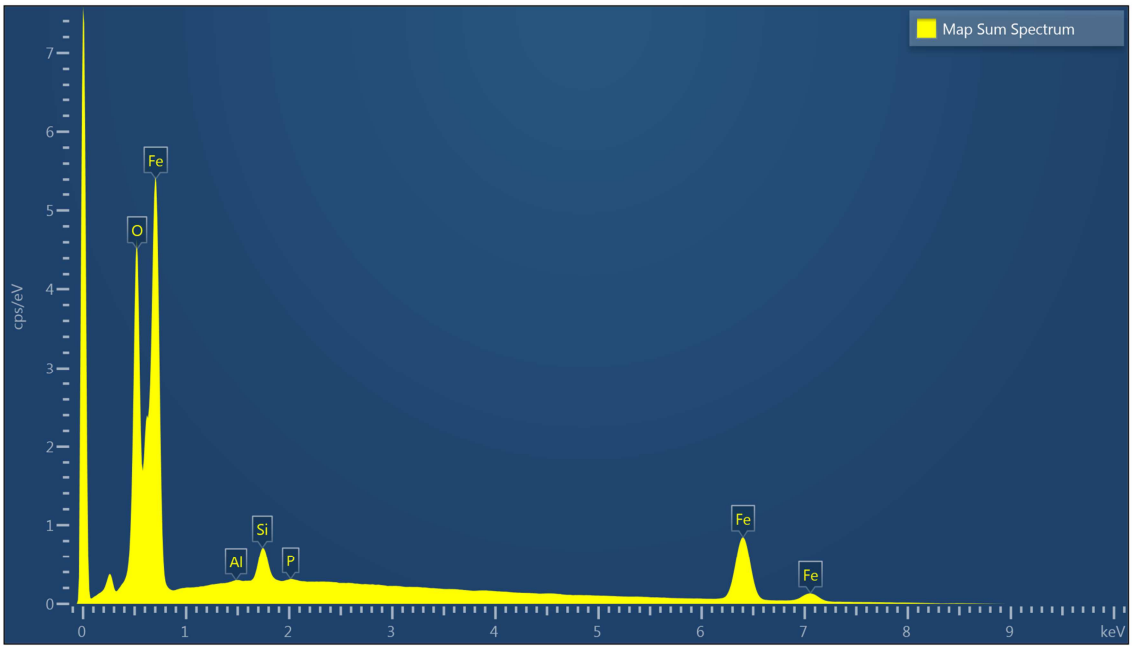

Figure A23. EDS spectrum of NANOFER STAR* nanopowder

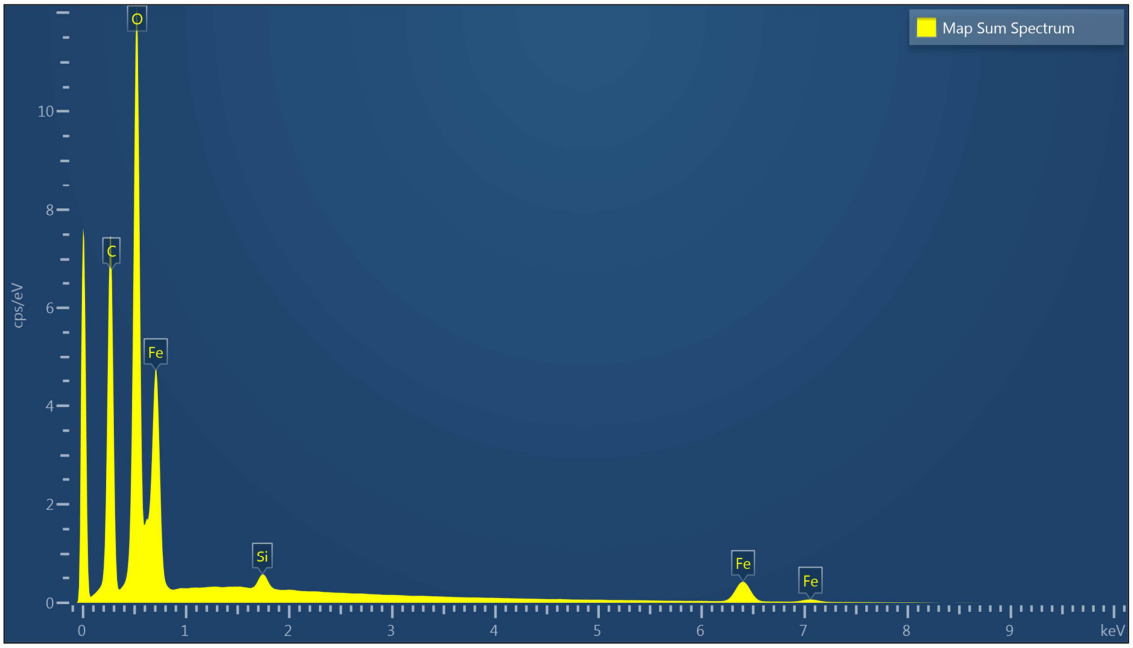

Figure A24. EDS spectrum of ferrihydrite nanopowder

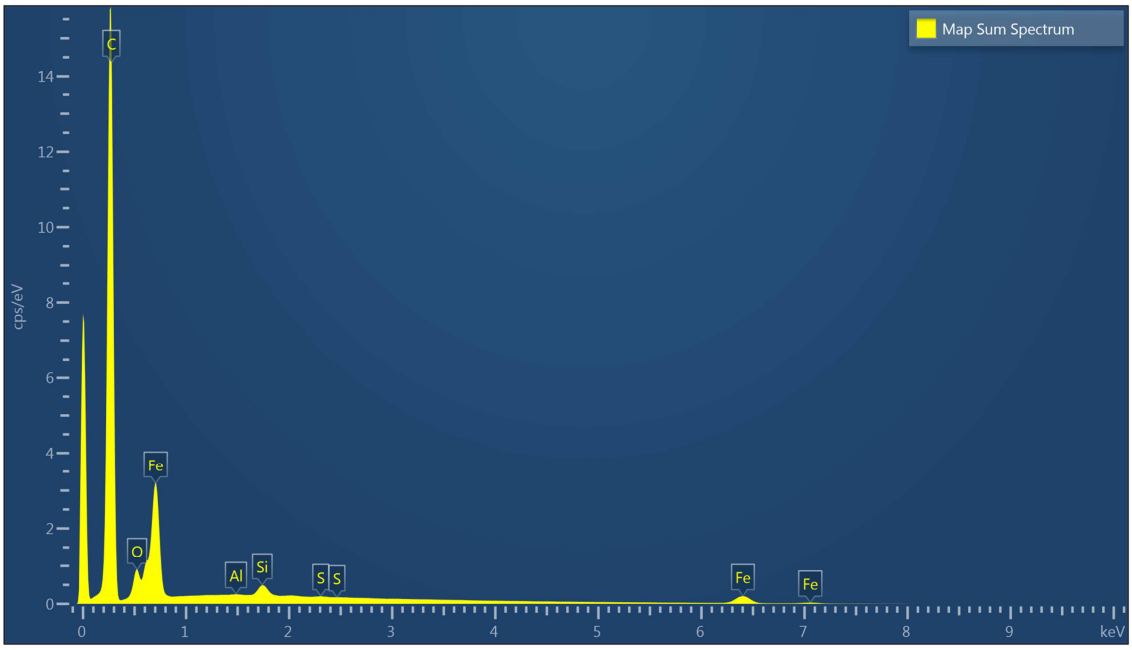

Figure A25. EDS spectrum of Carbo-Iron nanopowder

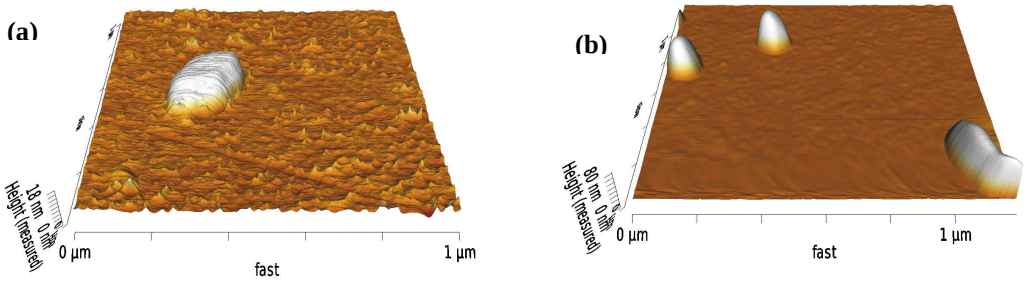

Figure A26. AFM 3D images of NANOFER STAR* from UPW and HRW: UPW (a); HRW (b).

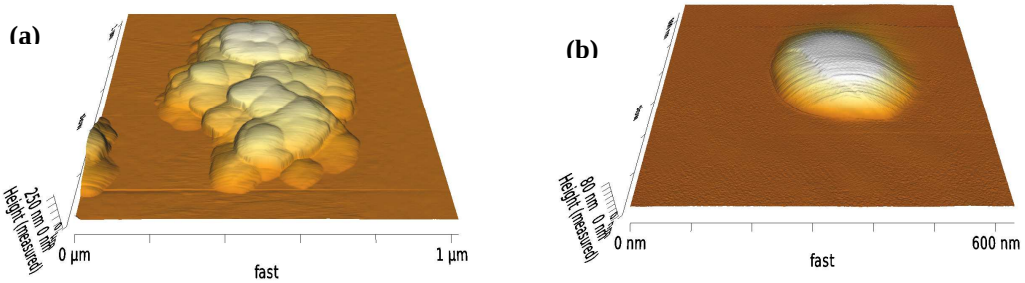

Figure A27. AFM 3D images of ferrihydrite from UPW and HRW: UPW (a); HRW (b).

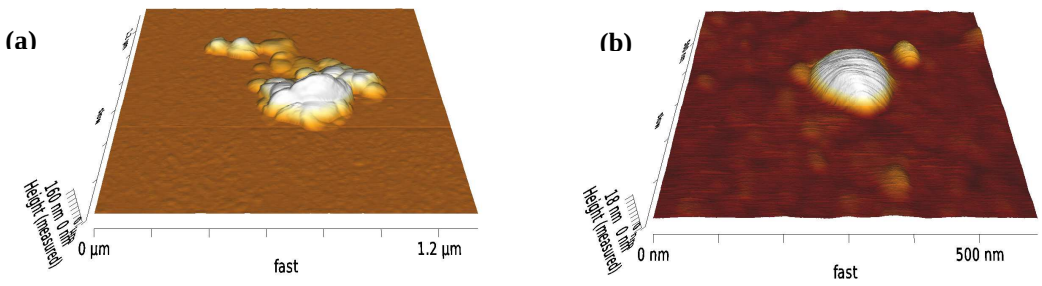

Figure A28. AFM 3D images of Carbon-Iron from UPW and HRW: UPW (a); HRW (b).